

# Spatial distribution models for the *Micrurus divaricatus* complex (Serpentes: Elapidae) in Nuclear Central America with emphasis on Honduras

Jorge Luis Montoya, Anthonie Ivanovich Andino-Mazariegos, Julio Enrique Mérida, and Gustavo Adolfo Cruz

Universidad Nacional Autónoma de Honduras, Museo de Historia Natural. Boulevard Suyapa, Tegucigalpa, Honduras.  
E-mail: [jlmontoya.jlmf@gmail.com](mailto:jlmontoya.jlmf@gmail.com).

## Abstract

**Spatial distribution models for the *Micrurus divaricatus* complex (Serpentes: Elapidae) in Nuclear Central America with emphasis on Honduras.** This study modeled the distribution of the *M. divaricatus* complex in Nuclear Central America (NCA) by testing multiple modeling techniques and identifying crucial bioclimatic predictors. We used 178 occurrence records and seven variables selected for ecological relevance and low collinearity. Validating the eight techniques using AUC, TSS, Cohen's Kappa, sensitivity, specificity, COR, and CA. Random Forest, Support Vector Machines, Generalized Additive Models, and Maximum Entropy Modeling performed best, with Random Forest showing the highest predictive accuracy. Main predictors were temperature seasonality, precipitation of the driest month, and precipitation seasonality. Projections indicated high suitability along the Pacific and Caribbean slopes and in parts of the Mosquitia, and low suitability in the Chortís Block highlands. Lowland and premontane moist forests were identified as critical habitats. The Chortís Block highlands represent a transitional zone for the three subspecies. These results, obtained via a multi-model approach to reduce uncertainty, provide relevant insights for taxonomy and conservation planning of the *M. divaricatus* complex and the genus *Micrurus* in NCA.

**Keywords:** *Micrurus divaricatus* complex, Nuclear Central America, Species distribution models.

## Resumen

**Modelos potenciales de distribución espacial para el complejo *Micrurus divaricatus* (Serpentes: Elapidae) en Centroamérica Nuclear con énfasis en Honduras.** Este estudio modeló la distribución del complejo *M. divaricatus* en Centroamérica Nuclear (CAN) mediante la evaluación de múltiples técnicas de modelización e identificación de predictores bioclimáticos cruciales. Se utilizaron 178 registros de ocurrencia y siete variables seleccionadas por su relevancia ecológica y baja colinealidad. Validando las ocho técnicas con las métricas AUC, TSS, Kappa de Cohen, sensibilidad, especificidad, COR y CA. Random Forest, Support Vector Machines, Generalized

Received 30 September 2024

Accepted 30 April 2025

Distributed December 2025

Additive Models y Maximum Entropy Modeling mostraron mejor desempeño, destacando Random Forest por su mayor precisión predictiva. Los predictores más importantes fueron la estacionalidad de la temperatura, la precipitación del mes más seco y la estacionalidad de la precipitación. Las proyecciones indicaron alta idoneidad en las vertientes del Pacífico y Caribe y en partes de la Mosquitia, mientras que se predijo baja idoneidad en las tierras altas del Bloque Chortís. Los bosques húmedos de tierras bajas y premontanos fueron identificados como hábitats críticos. Las tierras altas del Bloque Chortís representan una zona de transición para las tres subespecies. Estos resultados, obtenidos mediante un enfoque multimodelo reduce la incertidumbre, proporcionan información relevante para la taxonomía y la conservación del complejo *M. divaricatus* y género *Micrurus* en CAN.

**Palabras claves:** Centroamerica Nuclear, Complejo *M. divaricatus*, Modelos de distribución de especies.

### Resumo

**Modelos de distribuição espacial para o complexo *Micrurus divaricatus* (Serpentes: Elapidae) na América Central Nuclear com ênfase em Honduras.** Este estudo modelou a distribuição do complexo *M. divaricatus* na América Central Nuclear (CAN) testando múltiplas técnicas de modelagem e identificando preditores bioclimáticos chave. Foram utilizados 178 registros de ocorrência e sete variáveis selecionadas por relevância ecológica e baixa colinearidade Validando as oito técnicas usando AUC, TSS, Kappa de Cohen, sensibilidade, especificidade, COR e CA. Random Forest, Support Vector Machines, Generalized Additive Models e Maximum Entropy Modeling apresentaram melhor desempenho, com Random Forest mostrando a maior precisão preditiva. Os preditores principais foram a sazonalidade da temperatura, precipitação do mês mais seco e sazonalidade da precipitação. As projeções indicaram alta adequação ao longo das encostas do Pacífico e Caribe e em partes da Mosquitia, e baixa adequação nas terras altas do Bloco Chortís. Florestas úmidas de baixas altitudes e premontanas foram identificadas como habitats críticos. As terras altas do Bloco Chortís representam uma zona de transição para as três subespécies. Estes resultados, obtidos via abordagem multimodelo para reduzir a incerteza, fornecem informações relevantes para a taxonomia e conservação do complexo *M. divaricatus* e do gênero *Micrurus* na CAN.

**Palavras-chave:** América Central Nuclear, Complejo *M. divaricatus*, Modelos de distribuição de espécies.

## Introduction

Biological species modeling has become the primary statistical technique for predicting the potential distribution of a taxon by considering the abiotic and biotic conditions necessary for its establishment and persistence in a given territory (Guisan and Zimmermann 2000, Guisan and Thuiller 2005, Elith and Leathwick 2009, Mateo *et al.* 2011, Guisan *et al.* 2013, Elith and Franklin 2017). Species distribution models (SDMs) are a valuable tool for elucidating or anticipating the distribution patterns of a taxon. The development

of SDMs relies on the use of historical or contemporary occurrence records (coordinates/location), biotic and abiotic predictor variables, and elevation models (raster files) (Franklin 1995, Guisan and Zimmermann 2000, Phillips *et al.* 2006, Mateo *et al.* 2011, Elith and Franklin 2017).

The application of SDM has proven to be a valuable instrument for addressing problems at a systematic and taxonomic level by providing a quantitative and spatial framework for understanding the relationship between species and their environment (Lissovsky *et al.* 2021,

Rodríguez-Gómez *et al.* 2021). This assertion is supported by the proposal of biogeographic delimitations, thereby enhancing our comprehension of historical and evolutionary processes operating at the species and subspecies level (Rodríguez-Gómez *et al.* 2021). A key advantage of SDMs is their ability to identify new occurrence areas, significant transition zones, and critical regions for understanding the presence and movement patterns of these taxa (Mizsei *et al.* 2016). Furthermore, they help elucidate the factors influencing our understanding of ecological and morphometric variation in taxa. Consequently, they provide a comprehensive global perspective of the taxonomic landscape.

Beyond their ecological and taxonomic applications, SDMs play a crucial role in conservation planning and have significant implications for medical research. In regions with a high prevalence of venomous snakebites, they contribute to the development of conservation strategies, medical treatments, and preparation of antidotes (Fernández *et al.* 2011, Archis *et al.* 2018, Guerra *et al.* 2019, Rodríguez-Gómez, *et al.* 2021, Al Haidar *et al.* 2023, Jowers *et al.* 2023). Reptiles are a group of ectothermic organisms, comprising lizards, snakes, and turtles, that are currently facing challenges due to habitat alteration and destruction (Archis *et al.* 2018). A recent study by Biber *et al.* (2023) suggests a potential global decline in the richness of this group, based on an analysis of distribution patterns and bioclimatic variables. This analysis entailed the generation of 6,296 models for diverse reptile species, including 2,305 taxa classified within snakes. Understanding the distribution limits of a snake taxon is essential for analyzing biogeographic processes, ecological conservation, and medical relevance (Mota-Vargas and Rojas-Soto 2012, Archis *et al.* 2018, Guerra *et al.* 2019, Martín *et al.* 2022). Coral snakes represent a diverse group of species within the genus *Micrurus*, as classified by Wagler in 1824 (Roze 1982). Currently, approximately 85 species of *Micrurus* are

documented across the Americas (Jowers *et al.* 2023).

These snakes are distinguished by their distinctive coloration patterns in addition to their potent venom that is predominantly neurotoxic (Köhler 2003, Stazi *et al.* 2022). They belong to the Family Elapidae and exhibit a wide distribution in America, ranging from southwestern Oaxaca, Mexico, to northwestern Colombia (Roze 1996, Köhler 2008, McCranie 2011). This territory is inhabited by five distinct subspecies: *M. nigrocinctus babaspul* Roze, 1967, *M. nigrocinctus coibensis* Schmidt, 1936, *M. nigrocinctus divaricatus* Hallowell, 1855, *M. n. nigrocinctus* Girard, 1854, and *M. n. zunilensis* Schmidt, 1932. These subspecies display tricolor (red, yellow, and black) and bicolor (red and black) ring patterns, as documented by Köhler (2008) and McCranie (2011). Their diet consists of other snakes, lizards, and caecilians, and they reproduce via oviparous means. They exhibit a marked preference for dry forest, humid forest, and tropical rainforest habitats, with an altitude range of 0 to 1,640 m a.s.l. (Roze 1996, Köhler 2003, Köhler 2008, McCranie 2011).

Currently recognized as *Micrurus nigrocinctus* (Girard, 1854), this species is considered a complex (Köhler 2003, 2008, Campbell and Lamar 2004, Fernández *et al.* 2011, McCranie 2011, Jowers *et al.* 2023). A phylogenetic analysis conducted by Jowers *et al.* (2023) proposed three lineages. The first lineage includes the *M. nigrocinctus nigrocinctus* populations from Panama. The second lineage contains *M. nigrocinctus divaricatus* and *M. ruatanus* Günther, 1895 from Honduras. The third lineage comprises *M. nigrocinctus zunilensis* and *M. nigrocinctus nigrocinctus* populations from Chiapas, Guatemala, Honduras, Nicaragua, and Costa Rica. Notably, the first lineage exhibits a significant degree of genetic divergence from lineages two and three. According to the findings of Jowers *et al.* (2023), no specific taxonomic classification exists for Nuclear Central America (NCA) populations due to the presence of genetic evidence indicating

that *Micrurus nigrocinctus* Girard, 1854 is restricted to Panamá. Meanwhile, the second and third lineages represent a subspecies complex whose nominal status remains undetermined (for further details, please refer to Figure 2 in Jowers *et al.* 2023).

Consequently, the NCA populations are classified as a subspecies complex that currently lacks a taxonomic species designation and will henceforth be referred to as the *M. divaricatus* complex. This designation is because the name *M. divaricatus* was first used by Hallowell in 1854, making it the oldest name among these lineages. Given the absence of a well-defined classification system for this taxon in southern Mexico and Central America, the study species will be informally treated at the level of the previously used name *Micrurus divaricatus* Hallowell, 1854.

Several studies have focused on distribution modeling for different species of *Micrurus* (Terribile *et al.* 2007, Archis *et al.* 2018, Hidalgo-García *et al.* 2018, Guerra *et al.* 2019, Lara-Galván *et al.* 2023), particularly in context of NCA, according to the work of Hidalgo-García *et al.* (2018) and Lara-Galván *et al.* (2023). This genus holds both medical and taxonomic significance, as evidenced by the proposal of multiple lineages for NCA by Jowers *et al.* (2023). Developing distribution models for the *M. divaricatus* complex is highly valuable, as it enhances the current understanding of the generic distribution across the Americas. It also plays a crucial role in identifying suitable areas, areas with potential new records, and bioclimatic and ecological factors, which are essential for future studies of the *M. divaricatus* complex in NCA.

The objective of this study is to develop a distribution model for the *M. divaricatus* complex in NCA, with a particular focus on Honduras, given that the three subspecies comprising this complex are found in that country, along with an abundant number of presence records for these taxa. The study will entail a comparison of different algorithms for

the generation of SDMs, with the objective of selecting the techniques with the best performance in function of predictive variables according to bioclimatic and ecological aspects that contribute to the explanation of the distribution of the *M. divaricatus* complex, as well as detecting the bioclimatic variables and ecological aspects that influence this group of snakes.

## Materials and Methods

### Study Area

The study area was defined as the zone extending eastward from the Isthmus of Tehuantepec and the mountainous region of Chiapas (southern Mexico), Guatemala, El Salvador, and Honduras, encompassing the depression of Nicaragua between the Santa Elena Peninsula and the Hessian Escarpment. This region is geologically part of the Maya and Chortís blocks. The Nuclear Central America region is situated between the North American and Caribbean Plates (Figure 1) (Brineman and Vinson 1961, Savage 1966, Banks 1975, Donnelly *et al.* 1990, James 2007, Marshall 2007, Cano *et al.* 2018).

This region is a suitable area for the study of venomous snakes because it is considered a historical transition zone with remarkable richness and diversity, being an area of importance for the endemism of this reptile group in the Americas (Russell *et al.* 1997, Köhler 2003, Mata-Silva *et al.* 2019). Consequently, the generation of SDMs on *M. divaricatus* in this area contributes new information about historical, ecological, and evolutionary biogeographic patterns in this reptile group, specifically for the genus *Micrurus* and this subspecies complex. The existence of a significant number of catalogued records in museums, private collections, and numerous bibliographic references for this region facilitates the generation of SDMs that allow us to obtain more precise and rigorous results.

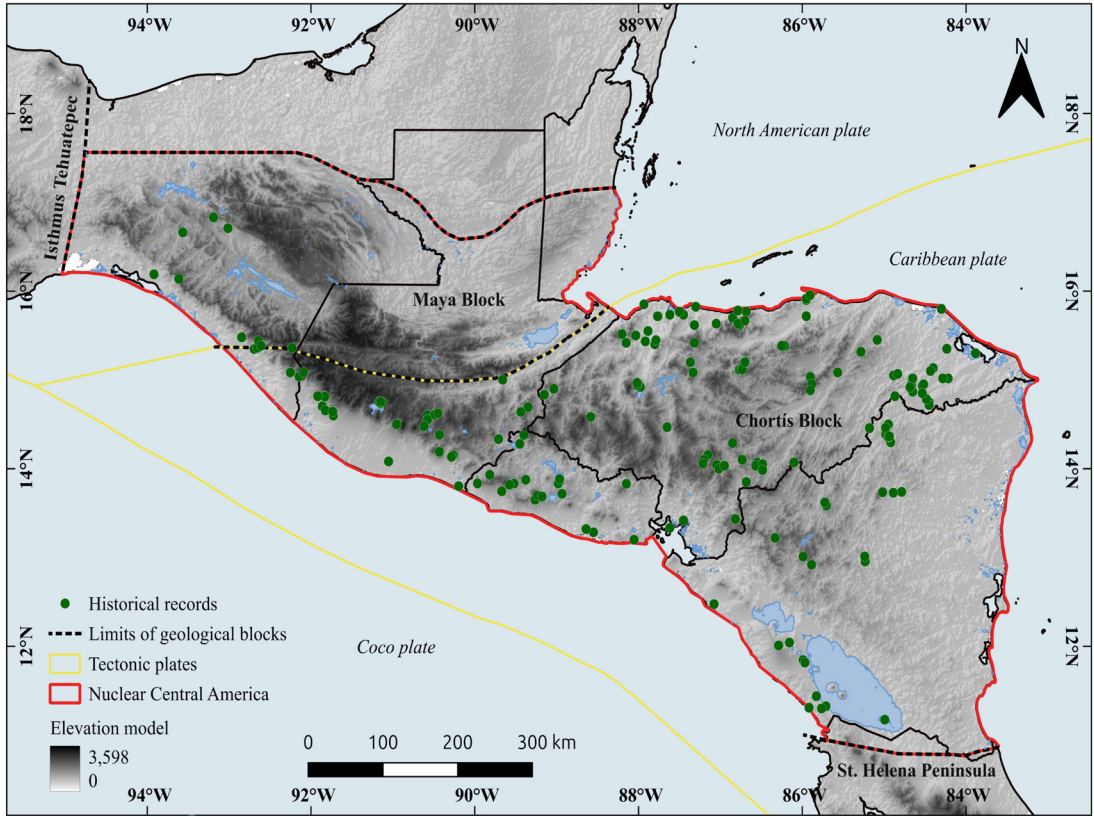


**Figure 1.** Historical records of the study species in NCA and delimitation of the Mayan and Chortís geological blocks. Map generated in QGIS 3.28.

### Occurrence Records

To obtain the georeferenced occurrence records of the study species, several databases were consulted: VertNet.org, 2016, (<http://portal.vertnet.org/search>); Global Biodiversity Information Facility, 2023 (GBIF.org, <https://www.gbif.org/>); Portal de Biodiversidad de Guatemala (<https://biodiversidad.gt/portal/index.php>) (Orellana and López 2023). The latter digital platform links to databases of the reptile collections of the University of Michigan Museum of Zoology UMMZ-Vertebrates, Smithsonian National Museum of Natural History NMNH-Vertebrates, University of Texas-Arlington

Herpetology UTA, Universidad del Valle de Guatemala UVG-UVGR, American Museum of Natural History AMNH-Vertebrates, Field Museum of Natural History FMNH-Zoology, Florida Museum of Natural History UF-Vertebrates, Museum of Comparative Zoology, Harvard University MCZ-Vertebrates, Museum of Vertebrate Zoology, University of California Berkeley MVZ-Herp, Muséum National d’Histoire Naturell MNHN-Vertebrates and Natural History Museum (London) NHM-Vertebrates; Taxonomic Catalog of the Biota of Mexico [CONABIO (comp) 2023], (<https://www.snib.mx/taxonomia/descarga/>). The following records were considered: those with specimens

conserved in museums, private biological collections, and data cited in scientific articles, as well as records of specimens deposited by one of the authors in the Museum of Natural History of the Universidad Nacional Autónoma de Honduras.

Appropriate records were considered to be data with the following considerations: (1) data with vouchers in biological collections, with catalog number of or collector code; (2) data with a geographical reference or a detailed description of the collection location; (3) records cited in scientific papers that have not yet been deposited in biological collections nor available in online databases, but which have been published in prestigious journals on this group. Data with only observation records were excluded. The selection of reliable records for the study area serves to eliminate the possibility of bias due to misidentifications that can occur in the various digital platforms that publish visual records.

The selected data were stored in a spreadsheet containing the following fields: a numerical code, the country or region of collection, geographic reference (longitude, latitude, in decimal degrees), and a bibliography of reference of the specimen record (Appendix I). Subsequently, the geographic references were refined and corrected with the help of relevant publications, scientific research articles, and books that provided detailed descriptions of the localities where the specimens were collected (Schmidt 1932, 1933, Gaige *et al.* 1937, Smith and Taylor 1945, Landy *et al.* 1966, Roze 1967, 1982, 1996, Seib 1984, Köhler 2001, 2003, 2008, Jansen and Köhler 2003, Köhler *et al.* 2006, Sunyer 2009, Illescas *et al.* 2011, McCranie 2011, Scott *et al.* 2011, Travers *et al.* 2011, Jowers *et al.* 2023).

Using the geospatial software Quantum GIS 3.28 (QGIS Development Team 2023), Google Earth Pro (Google 2023), and ACME mapper 2.2. (ACME 2024), the geographic points were coupled in a vector layer of southern Mexico and Central America and a satellite imagery layer

(QuickMapServices add-on in QGIS) for verification and rectification of the localities and geographic references of each record. Those with anomalies or incorrect geographic references or data that could not be georeferenced were discarded. Data with duplicated geographic references were considered as one record.

### *Climate Variables*

The selection of bioclimatic variables was based on ecological factors such as temperature and precipitation, as indicated by Marques *et al.* (2006), Mizsei *et al.* (2016), and Archis *et al.* (2018). Temperature and precipitation have been identified as significant ecological and biological factors that influence ectothermic species and the composition of surrounding vegetation, highlighting their crucial role in environmental dynamics. This statement is corroborated by McCranie (2011), who notes that distribution of these species in Honduras is predominantly concentrated in lowland rainforest, lowland dry forest, premontane rainforest, premontane wet forest, premontane dry forest, and low montane rainforest. These formations are delimited based on Holdridge's classification of life zones, which are determined by mean annual temperature, mean annual precipitation, humidity, and altitude. Bioclimatic variables were used in potential distribution studies for species of the genus *Micrurus* in different regions of the Americas, including the southern United States, southern Mexico, Central America, Rio de Janeiro, and southeastern Brazil (Terribile *et al.* 2007, Archis *et al.* 2018, Hidalgo-García *et al.* 2018, Guerra *et al.* 2019, Lara-Galván *et al.* 2023).

Consequently, a set of 13 bioclimatic variables and a digital elevation model (DEM) were obtained. This set of predictor variables was reduced to seven through a process that included the selection of the most frequently used variables in previous studies on species of the genus (Terribile *et al.* 2007, Archis *et al.* 2018, Hidalgo-García *et al.* 2018, Guerra *et al.* 2019, Lara-Galván *et al.* 2023). The application of a

collinearity analysis used the pairwise correlation coefficient and the variance inflation factor (VIF) to mitigate the bias introduced by highly correlated variables (more details in the section on identification of collinearity of the predictor variables).

The analysis showed that the mean diurnal range, temperature seasonality, mean temperature of the driest quarter, annual precipitation, precipitation seasonality, precipitation of the warmest quarter, and precipitation of the driest month exhibited the lowest correlation values. Although prior research indicated that the mean annual temperature is a significant factor in the modeling for taxa in this genus, it was excluded due to its high correlation in relation to the other variables. Bioclimatic variable files and digital elevation models were obtained from Worldclim.org (<https://www.worldclim.org/data/index.html>) (Worldclim.org. 2023), “bio30s” and “elev30s,” both with a spatial resolution of 1 km<sup>2</sup> (Fick and Hijmans 2017). The files were edited by making a raster mask at geographic extent between longitudes -95°02'23.70" W, -83°07'08.36" E, and latitude 10°46'11.96" S, 17°33'41.65" N in the software QGIS. For each variable, all files had the same pixel size (30"), with a size of ≈0.93 km, in latitude orientation.

### *Pseudo-absence*

Pseudo-absences were created to meet the requirements of Species Distribution Models (SDMs) that need them. The criteria used for generating these pseudo-absences included: (1) utilizing occurrence records from other species within the same genus, as advised by Phillips *et al.* (2009); (2) identifying and considering regions lacking valid occurrence records, such as the eastern highlands of the Chiapas Mountains in southern Mexico (cf. Johnson *et al.* 2015 classification), southern Petén in Guatemala, and southern Belize (Cayo, Stann Creek, and Toledo), for Honduras based on the distribution of *M. divaricatus* and its relationship with the Holdridge life zones for Honduras, where this

complex is absent, as proposed by McCranie (2011). A manual procedure was employed to generate pseudo-absences at random in these zones. Vector layers delineating boundaries within the specified regions were utilized, and an elevation layer was used to restrict the generation of pseudo-absences to a higher range of 0 to 1,900 m a.s.l. These actions were executed in the QGIS program. (3) In addition, pseudo-absences were generated along the study area, with the help of the background function (SDM), through the eDist method, using the occurrence records and a layer stack of the predictive variables that had been previously selected. It was determined that all pseudo-absences situated within a 0.1° radius of each occurrence record should be excluded.

### *Modeling Process*

The processing and execution of the models was conducted using R project software, version 4.3.0 (R Core Team 2023), RStudio version 2023.6.1.524 (Posit Team 2023), through the SDM package (Naimi and Araújo 2021). This package allowed adaptability in developing different modeling techniques and was flexible for generating SDMs, helping to reduce errors in the construction of species distribution models, as well as being easy to use (Naimi and Araújo 2016). The following steps were applied: (1) data loading into the RStudio interface (occurrences, pseudo-absences, and predictor variables); (2) identification collinearity of the predictor variables; (3) model processing, fitting, and evaluation; and (4) generation and preparation of predictions.

*Data import into the RStudio interface.*—The occurrence, pseudo-absence, and predictor variables (climatic) records were loaded into the RStudio interface. The predictor variables were then grouped into an ensemble file using the raster package (Hijmans 2023). The occurrence and pseudo-absence data were subsequently identified in a binary manner (1 = occurrence

and 0 = pseudo-absence) and converted to SpatialPointsDataFrame format using the “coordinates” function (sdm package).

*Identification of collinearity of the predictor variables.*—Typically, a threshold of VIF < 10 is used for the exclusion of correlated variables (Dormann *et al.* 2013, Naimi *et al.* 2013, Mpakairi *et al.* 2017, Arenas-Castro *et al.* 2022). Cobos *et al.* (2019) employed a different approach by setting the threshold at VIF < 5, which prompted a review of alternative cutoffs to assess their impact on model performance. To this end, a series of multicollinearity analyses were conducted, examining the impact of various VIF thresholds (VIF < 3, VIF < 5, VIF < 7, and VIF < 10) in the set of 14 pre-selected variables. These analyses indicated that the elimination of predictor variables with VIF values greater than 3 significantly reduced the set of predictor variables and decreased the performance of the models.

Analyses employing VIF < 5 and VIF < 7 thresholds identified the same set of predictor variables, with models exhibiting moderate performance in comparison to exclusion with a VIF threshold < 3. The set of predictor variables obtained in the analysis at a threshold of VIF < 10 exerted a favorable influence on model performance. Each set of predictive variables obtained at different VIF thresholds is evaluated by the performance of the models, using the sensitivity and specificity metrics.

This process allowed selection of the most optimal threshold, which groups the best set of variables. Consequently, the optimal threshold for excluding predictor variables with a high degree of correlation was determined to be a threshold of VIF < 10. During this last analysis, the variables BIO2, BIO4, BIO9, BIO12, BIO15, and BIO18 were not excluded on the basis that they are regarded as essential bioclimatic variables within the genus. The “sdmata” object was then constructed, containing information on occurrences, pseudo-absences in binary form, and predictor variables. For these analyses, the

“vifstep” function of the USDM package (Naimi 2023) was used to identify variables with high correlations, and the “keep” argument was utilized for the set of variables that should not be excluded. This function facilitates identification of collinearity between predictor variables through the use of VIF, an effective method to elucidate the relationship between a variable and multiple variables considered in the development of SDMs (Dormann *et al.* 2013, Naimi and Araújo 2016).

*Processing, model fitting, and evaluation.*—A wide variety of techniques is available for the development of SDMs. Elith *et al.* (2006), Plissock and Fuentes-Castillo (2011), Guisan *et al.* (2017) and Hijmans and Elith (2017) classified them into the following three groups: (a) profile or “envelope” methods: based on ranges of minimum and maximum values of climatic variables and values in the location of known occurrences, or mathematical distances to determine the possible occurrence of a species in an established area; (b) regression-based: this technique makes use of occurrence and absence data through multiple regressions, logistic regression, or poisson regression, and describes the relationship between predictor variables, occurrence, and absence; (c) machine learning: uses occurrence data, background data or absence/pseudo absence, predictive variables; within this group there are different techniques, some based on clustering trees and regressions, maximum entropy, and finally, a combination of simple linear method, regression, and outlier detection and class categorization such as support vector machines.

Among the profiling methods, the Bioclim (BIOC), Domain (DOM), and Mahalanobis (MAH) approaches were considered. The Bioclim method employs a straightforward algorithm based on Boolean operators (Busby 1991). In contrast, the Domain (Carpenter *et al.* 1993) and Mahalanobis (Mahalanobis 1936) methods rely on mathematical distances and the similarity of climatic characteristics to identify

potential new locations for occurrence (Elith *et al.* 2006, Hernández *et al.* 2006, Guisan *et al.* 2017). Conversely, regression techniques are predicated on the analysis of the relationship between occurrence data and predictor variables using regression methods. The following methodologies were employed: the generalized linear model (GLM) and the generalized additive model (GAM) (Guisan *et al.* 2002, Elith and Franklin 2013, Guisan *et al.* 2017). The machine learning approach entailed the implementation of random forest (RF), support vector machines (SVM), and maximum entropy modeling (MaxEnt) methods. These models are founded on the principles of classification and regression trees (Breiman 2001). The SVM technique can be applied to regression analysis, outlier detection, and class categorization to predict the areas of presence (Tax and Duin 2004, Guo *et al.* 2005, Hijmans and Elith 2017). According to Zhang and Li (2017), MaxEnt is an approach that employs a maximum entropy framework to contrast presences with predictor variables and to similarly consider absences. This allows the classification of areas with potential presence or absence of a taxon (Phillips *et al.* 2006, Hernández *et al.* 2006, Dudík *et al.* 2007, Guisan *et al.* 2017).

The eight modeling techniques described above were used for the modeling of *M. divaricatus*, with the algorithms for Bioclim, Mahalanobis, and Dominance being those fitted in the Dismo package (Hijmans *et al.* 2023) and MaxEnt implemented using the same framework as the Java package 'MaxEnt', version 3.4.0. While each modeling technique makes different assumptions based on their algorithms when generating SDMs, it is important to review the predictive response from different approaches due to the high environmental, biogeographical, and dataset variation obtained for the study area. This also allows the selection of models that reveal more suitable information for the distribution of this complex. The predictive responses are evaluated using the most common statistics in the evaluation of SDMs (Shabani *et*

*al.* 2018), allowing us to identify the best model to fit our data and study area.

They also allow for an assembly of the models with the best predictive responses, grouping areas with better suitability and reducing the uncertainties of the different models (Araujo and New 2007, Thuiller *et al.* 2009). This approach will provide more robust boundaries of the distribution of the *M. divaricatus* complex in NCA. The following structure was used for each modeling technique: "sdm(bi~BIO2+BIO4+BIO9+BIO12+BIO14+BIO15+BIO18, data = "Presence - Pseudoabsence," methods = "Models," dep.test, replication = boot,  $N = 10$ )" modifying only the "methods" argument. The "sdm" function (sdm package) was used to fit the models, and replications of the different models were performed using the bootstrap method.

To validate the models, a subset of the data prepared for training the models was selected using the bootstrapping technique. This was done to perform validation with dependent test data and to determine the proportion of test data to be used for validating the different models under consideration. Publications on SDMs have proposed that the proportion of test data should be within the range of 20% to 40% for this purpose (Hidalgo-García *et al.* 2018, Stevens and Conway 2019, Interiano *et al.* 2024, Montero and Velasco 2024). In accordance with the aforementioned guideline, five models were executed with test data partitions of 20%, 25%, 30%, 35%, and 40%, comprising 10 replication iterations and 100 repetitions for each modeling method. The models generated with varying percentages of test data partitions were evaluated using the following metrics: the area under the ROC curve (AUC), the true skill statistic (TSS), and the point-biserial correlation coefficient (COR). For each technique, the test data proportions yielding the highest mean values for these metrics were selected, employing the criterion  $\max(\text{se} + \text{sp})$  as the threshold.

The statistical analyses employed to assess the adequacy of the various models were

executed using the “getEvaluation” and “evalates” functions of the SDM packages (Naimi and Araujo 2021). This assessment contributes to the calibration of the models, during which the aforementioned metrics, along with sensitivity and specificity, were employed. The integration of diverse metrics was based on prevalence (AUC and COR), threshold-independent, and threshold-dependent confounding matrix-based statistics (TSS, Kappa, Sensitivity and Specificity), enabling a more rigorous validation process and facilitating a multifaceted evaluation of the SDMs (Fielding and Bell 1997, Segurado and Araújo 2004, Allouche *et al.* 2006, Elith *et al.* 2006, Franklin 2009, Mouton *et al.* 2010, Naimi and Araújo 2016, Guisan *et al.* 2017, Shabani *et al.* 2018).

Considering optimal values between 0.8–0.89 as good, values above 0.9–0.99 are considered very good, and 1 as perfect, for AUC, in the case of TSS and Kappa  $\geq 0.7$ –0.79 good, 0.8–0.99 very good, and 1 perfect, while sensitivity and specificity range between 0–1, with  $\geq 0.8$ –1 being acceptable values, for COR and CA close to 1 (Vaughan and Ormerod 2005, Pearson 2010, Phillips and Elith 2010, Zhang *et al.* 2015, Komac *et al.* 2016, Guisan *et al.* 2017). During the evaluation processes, a total of 30 rounds of runs were executed. These consisted of adjusting the number of pseudoabsences required and the selection of predictor variables at different VIF thresholds (VIF < 3, VIF < 5, VIF < 7, VIF < 10), according to the values of the metrics established, considering the number of pseudoabsences and the VIF threshold with optimal results for the different models. In addition, the variables with the highest relative importance and response were calculated with AUC, using the “rcurve” and “getVarImp” functions (SDM package).

*Elaboration of predictions and maps.*—Eight predictions for the considered models were generated using the “predict” function (SDM package), from the average of the ten models corresponding to each technique, with the following

structure: “predict (RF10, newdata = layer, mean = T).” In addition, an average prediction of the most efficient models was generated on a scale from 0 to 1 to delimit the zones of occurrence. Following the example of the method proposed by Hijmans and Elith (2017), modifying the threshold of 0.5 by an average value of the thresholds obtained by max (se+sp) for the considered models. Subsequently, a second validation was performed using the projections of the generated predictions (transformed to binary) and the occurrence and pseudo-absence data. The same metrics used in the initial evaluation were applied, augmented with the inclusion of the Kappa coefficient and the calibration statistic (CA). This was done to evaluate the discrimination and calibration of the predictions.

The calibration statistic was calculated according to the methodology described in the SDM package. The remaining metrics AUC, TSS, Kappa, COR, Sensitivity (SEN), and Specificity (SPE) were obtained using the “absence.accuracy” and “ecospat.meva.table” functions from the PresenceAbsence and ecospat packages (Broennimann and Di Cola 2023, Freeman 2023). The projections of predictions were selected based on the values resulting from the second round of evaluation. The coefficient of variation was calculated to illustrate areas of agreement between the models. This was achieved by utilizing the “cv” function (raster package). These projections were exported in TIF format using the “writeRaster” function (raster package) and processed in QGIS 3.22 to prepare the potential distribution maps of the *M. divaricatus* complex. The predicted area for Holdridge life zones (Holdridge 1978) for Honduras was also calculated from the average prediction of models with good performance on a scale of 0–1, according to the example presented by Hijmans and Elith (2017). With the help of geospatial tools and the Group Stats add-on in the QGIS program, the area of overlap of life zones and area of possible occurrence of the *M. divaricatus* complex was estimated. The

methodology described above is designed to align with the recommendations made by Zurell *et al.* (2020) during the development of SDMs. The objective is to facilitate the creation of more reliable, reproducible, and efficient models.

## Results

The models were derived from a dataset comprising 178 occurrence records obtained from the different localities in various countries (16 from southern México, 28 from Guatemala, 19 from El Salvador, 87 for Honduras, and 28 from Nicaragua) and 306 pseudo-absences, also generated for study area (97 from southern Mexico, 19 from Belize, 61 from Guatemala, 17 from El Salvador, 53 from Honduras, and 59 from Nicaragua). The collinearity analysis conducted on the 14 predictor variables, which were initially chosen based on studies of taxa from the genus *Micrurus*, identified six bioclimatic variables and the elevation model as having a high degree of correlation. As a result, these variables were excluded from further analysis, leading to the development of the models based on seven variables (BIO2, BIO4, BIO9, BIO12, BIO14, BIO15, and BIO18) and the dataset described above (occurrence and pseudo-absences).

The findings derived from the metrics employed during the model fitting and evaluation processes identified four models with acceptable performance levels. Among these, the RF model

stood out as the top performer, surpassing SVM, GAM, and MaxEnt. The RF model achieved values of AUC = 0.97, TSS = 0.86, and COR = 0.85, revealing very good performance. While the SVM, GAM, and MaxEnt models also demonstrated good performance with values of AUC  $\geq$  0.87, the rest of the metrics showed values of TSS  $\geq$  0.70 and COR  $\geq$  0.67, indicating good predictive capability. These values, collectively, indicate that all four models possess sufficient accuracy to forecast the potential distribution of the *M. divaricatus* complex. MaxEnt consistently exhibited lower TSS and COR values compared to the other three models (refer to Table 1).

The second evaluation of the generated predictions reinforced the initial results, with the RF model again demonstrating superior performance. It achieved the highest scores: AUC = 0.99, TSS = 0.91, Kappa = 0.89, COR = 0.90, CA = 0.75, SEN = 0.98, and SPE = 0.93, indicating very good predictive capacity. In comparison, the SVM and GAM models exhibited strong results across the board, with AUC  $\geq$  0.93, TSS  $\geq$  0.71, Kappa  $\geq$  0.66, COR  $\geq$  0.74, CA  $\geq$  0.84, SEN  $\geq$  0.88, and SPE  $\geq$  0.76, delivering good predictions. Meanwhile, MaxEnt demonstrated slightly weaker results with an AUC = 0.90, TSS = 0.66, Kappa = 0.63, COR = 0.68, CA = 0.84, SEN = 0.87, and SPE = 0.79. These metrics reflected satisfactory values for the MaxEnt models and demonstrated acceptable

**Table 1.** The values obtained in the first evaluation were based on a subsample of the training data for use in the validation of the different models, applying the AUC, TSS, and COR metrics. The best performing models are presented in bold. These acronyms are also used in the following sub-section: Processing, Model Fitting, and Evaluation.

	RF	SVM	GAM	MaxEnt	MAH	GLM	DOM	BIOC
AUC	<b>0.97</b>	<b>0.91</b>	<b>0.87</b>	<b>0.89</b>	0.91	0.80	0.76	0.73
TSS	<b>0.86</b>	<b>0.73</b>	<b>0.70</b>	<b>0.70</b>	0.67	0.57	0.46	0.41
COR	<b>0.85</b>	<b>0.72</b>	<b>0.69</b>	<b>0.67</b>	0.38	0.50	0.42	0.28
TH	0.44	0.31	0.52	0.46	-0.17	0.31	0.54	0.02

**Table 2.** The second evaluation yielded the following values, which were calculated using the prediction projections and the entire training data set for validation. The following metrics were applied: AUC, TSS, Kappa, COR, CA, SEN, and SPE. The best performing models are indicated in bold.

	<b>RF</b>	<b>SVM</b>	<b>GAM</b>	<b>MaxEnt</b>	<b>MAH</b>	<b>GLM</b>	<b>DOM</b>	<b>BIOC</b>
AUC	<b>0.99</b>	<b>0.93</b>	<b>0.97</b>	<b>0.90</b>	0.93	0.79	0.76	0.73
TSS	<b>0.91</b>	<b>0.71</b>	<b>0.72</b>	<b>0.66</b>	-0.04	0.54	0.30	0.38
Kappa	<b>0.89</b>	<b>0.66</b>	<b>0.70</b>	<b>0.63</b>	-0.03	0.49	0.29	0.33
COR	<b>0.90</b>	<b>0.74</b>	<b>0.84</b>	<b>0.68</b>	0.36	0.49	0.31	0.39
CA	<b>0.75</b>	<b>0.87</b>	<b>0.84</b>	<b>0.84</b>	-0.02	0.77	-0.17	0.76
SEN	<b>0.98</b>	<b>0.94</b>	<b>0.88</b>	<b>0.87</b>	0.95	0.89	0.66	0.84
SPE	<b>0.93</b>	<b>0.76</b>	<b>0.84</b>	<b>0.79</b>	0.01	0.65	0.64	0.54

performance. Nevertheless, the slightly lower values suggest reduced predictive accuracy compared to the other three models (Table 2).

The evaluations underscored the importance of utilizing a diverse range of metrics such as AUC, TSS, Kappa, COR, SEN, and SPE for a more holistic and rigorous assessment through tailored statistical methodologies specific to each metric. For instance, the MAH model demonstrated suboptimal performance for COR and CA values despite achieving high scores for metrics like AUC, TSS, and Kappa. Models where SPE exceeded SEN were deemed less favorable (Tables 1 and 2). Similarly, models such as Bioclim, Domain, and Generalized Linear Model were excluded due to their failure to meet optimal criteria across these metrics. These models produced inaccurate and low-quality predictions regarding the distribution of the *M. divaricatus* complex, further validating the significance of this multi-metric approach in model evaluation. During these validations, various proportions of test data were assessed to determine optimal performance levels. The analysis suggested that the following percentages of test data delivered the best results: 20% MAH, 30% for RF and BIOC, 35% for GAM, GLM, and DOM, 40% for SVM and MaxEnt (Appendix II). Although performance differences

across these percentages were minimal, the models showed their highest accuracy within these ranges. This was demonstrated by the average values recorded for key metrics such as AUC, TSS, and COR (refer to Appendix II for statistics).

Projections from various models revealed significant differences in how this complex is distributed. This can be seen through the values of the coefficient of variation obtained from predictions made by RF, GAM, and MaxEnt (Figure 2). The MaxEnt model primarily shows a Pacific prevalence for NCA, with areas of moderate to high suitability. The Sierra Madre de Chiapas displayed less suitability, characterized by low values. Conversely, the highlands of the Chortís Block in Honduras and Nicaragua projected areas with low suitability. In contrast yet again, the Caribbean slope regions of Honduras exhibited high suitability, while the Honduran Mosquitia and Nicaraguan Mosquitia regions presented areas of half suitability (Figure 3A). In contrast, the RF model showed a reduction in areas corresponding to the highlands of the Chortís block, with low suitability values. The Pacific slopes of Nicaragua exhibited larger areas with low and medium suitability, with certain specific zones of high suitability such as the Pacific coast of El Salvador. Similar patterns

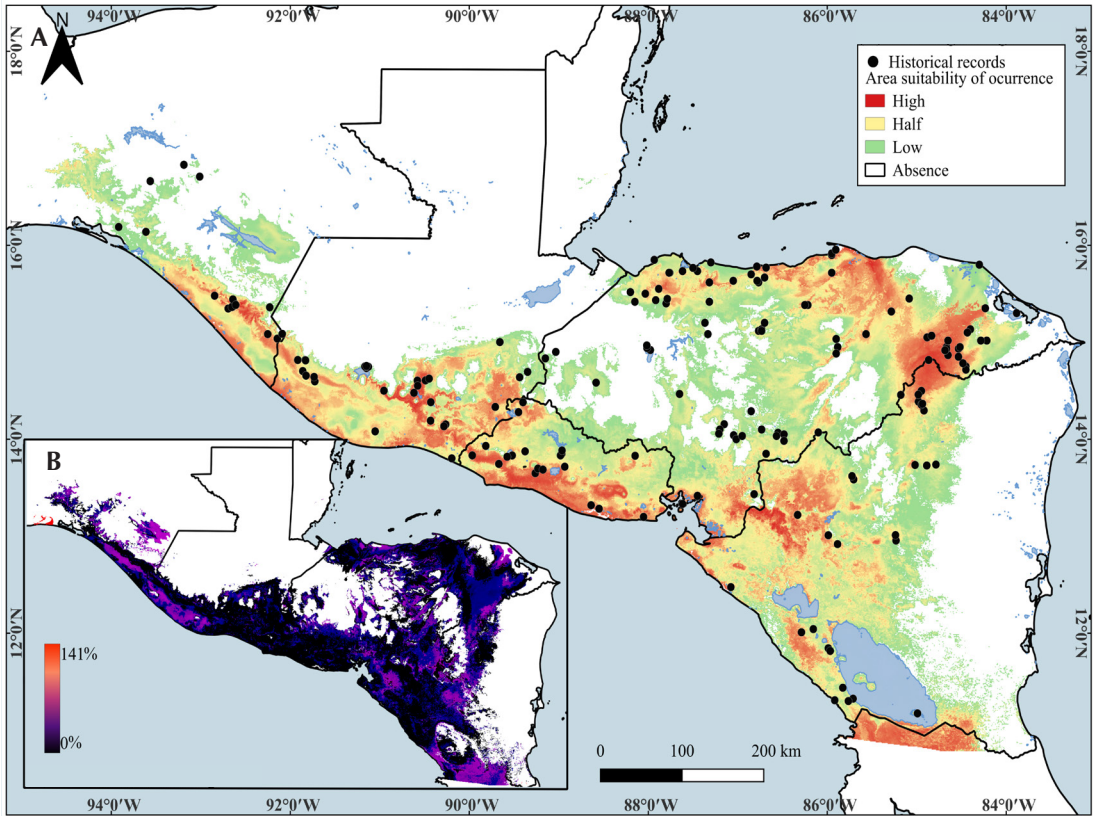


**Figure 2.** (A) Projected average of the RF, GAM, and MaxEnt models, along with historical records for the *M. divaricatus* complex in the NCA. (B) Coefficients of variation for the suitability areas indicated by the models.

were observed for the Caribbean slope of Honduras and the Mosquitia region, where the lowlands showed high suitability (Figure 3B).

The SVM model presented a distribution similar to MaxEnt, but it indicated larger areas with high suitability for the Pacific slope of NCA and an increase in suitable areas with low values in the Sierra Madre de Chiapas. On the other hand, the lowlands of the Caribbean side of Honduras and the Mosquitia revealed high suitability. Meanwhile, the highlands of the Chortís block projected a broad area of low suitability values for Honduras and high suitability in the Chortís lands of Nicaragua (Figure 3C). This model identified a small area of suitability conditions in the highlands of

Belize. The GAM model produced a varied distribution of areas with values ranging from low to medium and high suitability. The regions demonstrating favorable suitability for the presence of this complex are consistent, both on the Pacific slope and in the Caribbean areas of Honduras and Mosquitia. Notably, the Chortís block region exhibited a broad area of high suitability, contrasting with projections from MaxEnt, RF, and SVM models.

This model acknowledged favorable suitability areas in the Belize highlands and predicted high suitability in the Sierra Madre de Chiapas and the Chiapas highlands (Figure 3D). Areas identified with negative suitability included the northern Sierra Madre Mountains in Chiapas,

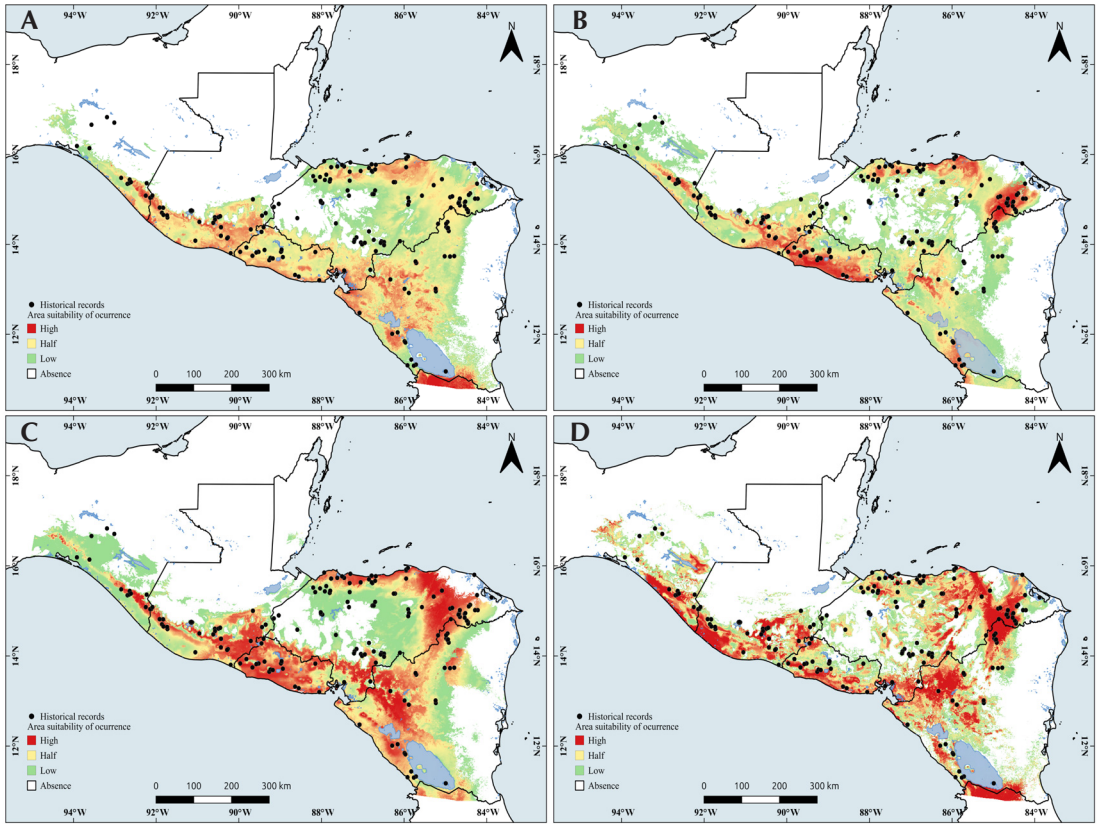


**Figure 3.** Predictions of the potential distribution of *M. divaricatus* complex in NCA using MaxEnt (A), RF (B), SVM (C), and GAM (D). Map generated in QGIS 3.28.

southern Belize, the Petén highlands, the high mountains of Guatemala, the region north of the Polochic-Jocotán and Motagua faults, and the northwestern Mosquitia region of Honduras. Sections of the Chortís Block highlands and most of the Caribbean coast of Nicaragua also displayed negative suitability. The differences in predicted distribution and suitability areas across the models highlight significant variability in estimating suitable regions for various ecosystems in Holdridge’s classification for Honduras.

Among the models analyzed, MaxEnt identified large regions of suitability for most ecosystems, including Lowland Arid Forest. It showed restricted suitability areas for Lower Montane Moist Forest. In contrast, the RF, SVM,

and GAM models exhibited a gradual reduction in the extent of suitable areas across the ecosystems. Premontane Moist Forests and Lowland Dry Forests were associated with a reduced portion of suitable areas in these models. The Lowland Arid Forest and Lower Montane Moist Forest displayed very minimal suitable regions. On the other hand, the Lowland Moist Forest demonstrated extensive suitability across all four modeling approaches, with only minor variation observed between models. This finding underscores the importance of the Lowland Moist Forest, likely serving as a critical ecosystem for the species complex within Honduras.

The overlap analysis of Holdridge life zones and the average projections generated by the RF,

GAM, and MaxEnt models provided an estimated area of overlap and potential habitat for these ecosystems in Honduras, relative to the distribution of the *M. divaricatus* complex. The results identified overlapping areas of 23,289.12 km<sup>2</sup> for Lowland Moist Forest, 10,135.04 km<sup>2</sup> for Lowland Dry Forest, 10,951.40 km<sup>2</sup> for Premontane Moist Forest, 17,622.18 km<sup>2</sup> for Premontane Wet Forest, 1,285.53 km<sup>2</sup> for Premontane Dry Forest, and 1,114.99 km<sup>2</sup> for Lower Montane Moist Forest. Collectively, these findings suggest that the *M. divaricatus* complex primarily spans six ecosystems within the Honduran territory, covering a potential area of 63,236.1 km<sup>2</sup>.

The assessment of response patterns to predictor variables across four modeling

approaches revealed that variables BIO4, BIO14, and BIO15 exert significant influence on the distribution of the *M. divaricatus* complex. While BIO12 notably impacted models generated by SVM, other predictor variables exhibited moderate effects. For the MaxEnt, SVM, and GAM, response values varied from 0.8 to 0.97, contrasting with RF, which exhibited a lower response value of 0.69 (Figure 4). In the analysis of variable importance, BIO4, BIO14, and BIO15 emerged as key factors for predicting the distribution of this complex. BIO4 was identified by RF, SVM, GAM, and MaxEnt as the variable with the greatest contribution in the distribution patterns generated by these approaches for the *M. divaricatus* complex (Figure 5). Additionally,

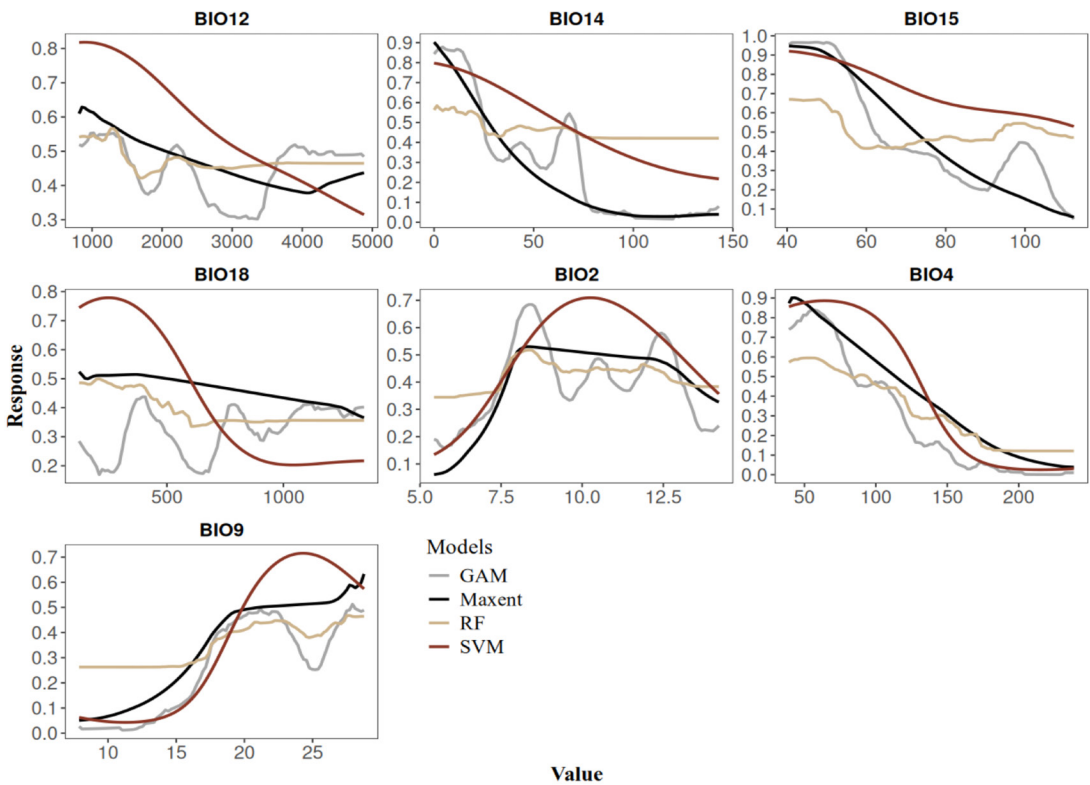


**Figure 4.** Illustrates the response curves that depict the influence of predictor variables in the top-performing models. The x-axis displays the values of these predictor variables, while the y-axis represents the response rate of the models on a scale from 0 to 1.

both GAM and MaxEnt underscored the relative importance of BIO14 and BIO15 over other variables. These findings indicate that BIO4, BIO14, and BIO15 are essential for comprehending the distribution patterns and ecological factors influencing the *M. divaricatus* complex. Furthermore, a set of preferred values was determined, which is favorable for the occurrence of this complex (for more details on these ranges, refer to Appendix III).

**Discussion**

The findings indicated that Random Forest (RF), Support Vector Machine (SVM), Generalized Additive Models (GAM), and

Maximum Entropy (MaxEnt) are the most effective tools for modeling the distribution of the *M. divaricatus* complex, with RF showing the highest performance. These outcomes align with other research studies on modeling techniques, such as those by Van Strien (2008) and Pliscoff and Fuentes-Castillo (2011). These approaches delimited an area of distribution which spans from the Isthmus of Tehuantepec to the end of the Nicaraguan depression. The models suggest a restricted distribution for the complex north of the Motagua-Polochic-Jocotán fault and predict lower distribution probabilities in the highlands of the Chortís block. They also identify high transition potential between the Pacific and Caribbean slope zones of both

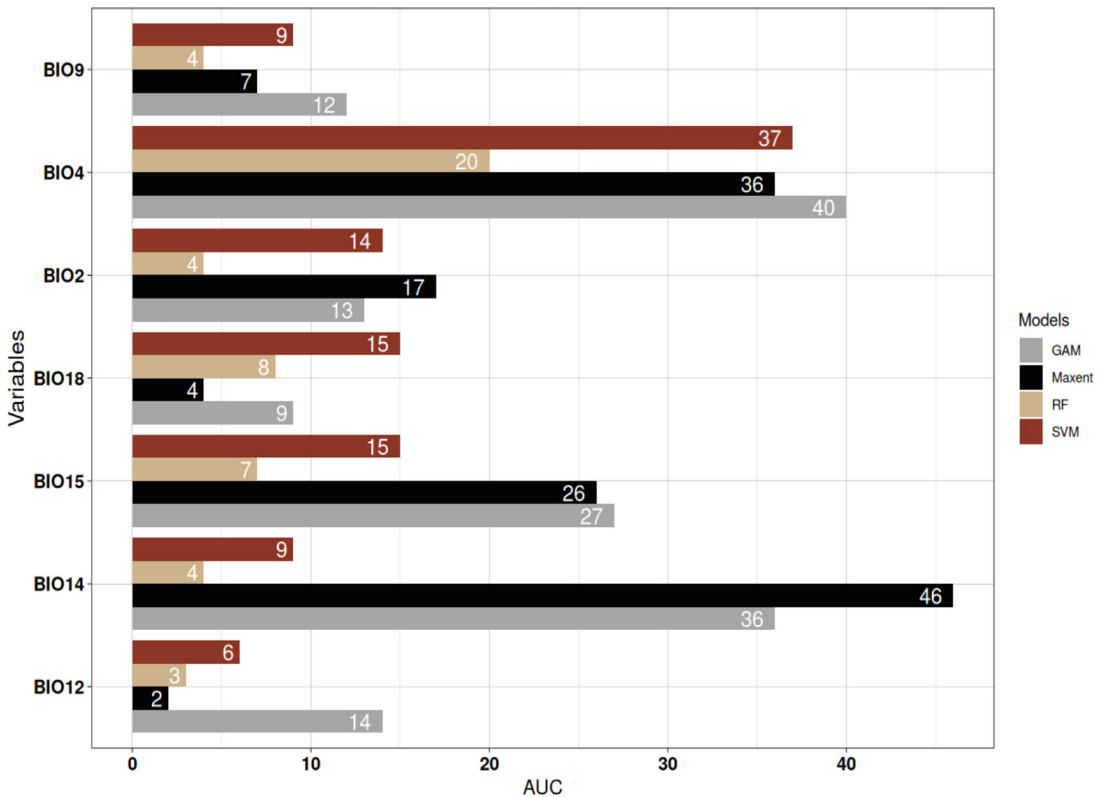


**Figure 5.** Displays the findings from analyzing the variables with the highest relative importance across four models that demonstrated strong performance for the *M. divaricatus* complex, using the AUC metric method. The bars illustrate the percentage contribution of each variable within these models.

Honduras and Nicaragua (Figure 2). RF, SVM, and GAM are found to more precisely define the distribution range, as the probabilities of presence decrease toward ecological boundaries compared to MaxEnt results.

All models consistently highlight the lowland and mid-elevation areas as particularly suitable for the occurrence of this complex, especially on the Pacific slope of NCA, the Caribbean slope of Honduras, and the Mosquitia regions in both Honduras and Nicaragua. In these locales, the combination of high temperatures and moderate precipitation seems favorable for the prevalence of these taxa. On the other hand, while the highlands of the Chortís block might significantly influence movement patterns, high precipitation levels could render these environments less suitable for occurrence. Similar challenges might arise north of the Motagua-Polochic-Jocotán fault, along Nicaragua's Caribbean coast, and in the highlands of Chiapas, where a disproportionate balance of temperature and precipitation likely restricts the presence of these species. This is supported by results regarding the response and significance of the bioclimatic variables employed.

In the context of this study, the variables BIO4, BIO14, and BIO15 showed valuable insights, suggesting a high likelihood that this complex is linked to NCA regions. This association is marked by BIO4 values ranging from 43.25 to 135.87, BIO14 values between 1.4 to 83.8, and BIO15 values spanning 40.5 to 112.3 (Appendix III). These parameters reflect the preference of the *M. divaricatus* complex for tropical rainforest and dry forest ecosystems, as previously documented by Köhler (2003) and McCranie (2011). These regions typically experience brief periods of seasonal rainfall, while temperatures seldom drop below 75.20 °F. Among these variables, BIO4 is considered crucial in explaining the distribution of the complex, though BIO14 and BIO15 also play significant roles in understanding the genus and distribution patterns of other taxa of *Micrurus*. This observation aligns with findings by Hidalgo-

García *et al.* (2018), who analyzed *M. diastema* (Duméril, Bibron, and Duméril, 1854) and *M. elegans* Jan, 1858 within the region.

Research conducted by Hidalgo-García *et al.* (2018) and Lara-Galván *et al.* (2023) on *M. diastema*, *M. elegans*, and *M. distans* Kennicott, 1860 revealed distribution patterns that align with the defined negative suitability zones for the *M. divaricatus* complex. Observed overlap occurs in the Maya Mountains region of Belize, the highlands of Chiapas, and the western Chortís Block. A more extensive overlap was identified west of the Sierra Madre and in the Pacific regions of Chiapas, near the Isthmus of Tehuantepec. These findings suggest that competitive interactions among these species may significantly impact their spatial boundaries in these areas. Further investigation is necessary to explore specific niche dynamics and ecological competition in regions where overlaps are most pronounced.

To confirm the effectiveness of our distribution models for this complex, field evaluations are recommended, following the methodology outlined by Mizsei *et al.* (2016). These evaluations involve field sampling to assess species presence and the functionality of predicted values in key areas, particularly those lacking previous records. This approach also aids in gathering new ecological data. Incorporating biotic variables could enhance predictive accuracy in certain regions, a factor not addressed in this study. Future research should explore the identification of abiotic and biotic tolerance ranges to achieve a more precise ecological characterization of this complex along the NCA corridor. Understanding these ecological relationships will clarify how they affect the distribution of each subspecies within the complex. Additionally, investigating the role of diet as a pivotal biotic factor influencing distribution is an important avenue for future studies.

In accordance with the aforementioned points, ascertaining dietary preference and levels of predation among the three subspecies within

the NCA biogeographic area could facilitate a more profound comprehension of their competitive feeding interactions and underscore regions exhibiting elevated predation rates. These factors are of paramount importance, as they contribute to ecological characterizations and facilitate a more precise delineation of the distribution of this species complex. Subspecies-level venom studies have the potential to identify unique taxonomic and ecological characteristics for each subspecies in this region. This research could provide valuable information for medical treatments by establishing toxicity levels and proteomic data among populations residing in Honduras. A salient example is the findings on *M. ruatanus* (Günther, 1895) (a population from the Caribbean islands of Honduras), which is believed to have evolved recently from *M. divaricatus* but shows a high toxicity level compared to other groups in Central America (Lippa *et al.* 2019, Jowers *et al.* 2023).

In accordance with the IUCN's 2024 classification system for species protection, this complex is currently designated as Least Concern (LC). This status is subject to re-evaluation in light of recent findings by Jowers *et al.* (2023). In Honduras and the nearby region, an alternative system focused on species protection is in place: the Environmental Vulnerability Score (EVS) proposed by Wilson and McCranie (2004). This system assigns a value of EVS = 9, placing it in the low range. Conversely, Johnson *et al.* (2015) have proposed an EVS value of 12 for NCA, which falls within the medium range. While the latter evaluation appears more suitable, it is recommended that the EVS for this species complex be re-evaluated, taking into account the level of subspecies as a criterion. This recommendation is because each subspecies may be subject to different types of negative impacts or a higher degree of vulnerability in various regions of NCA. This species complex exhibits an intriguing genetic richness, and it would be beneficial to expand the components of the EVS by including the significance of the genetic pool

presented by the subspecies within a taxon.

The differences observed between the models highlight the importance of integrating multiple approaches when studying species distributions, which helps reduce uncertainty in the final projection for a taxon. The results indicate that the bioclimatic variables Temperature Seasonality (BIO4), Precipitation of Driest Month (BIO14), and Precipitation Seasonality (BIO15) are essential for understanding the ecological distribution and characterizations of the *M. divaricatus* complex in NCA. The overlapping ecosystems and spatial distribution reaffirm the significance of Lowland Moist Forest and Premontane Moist Forest as critical ecosystems and habitats for this species complex. This information is crucial for ecological conservation and management, emphasizing the need to protect these types of forests. Considering the historical distribution patterns proposed by Campbell and Lamar (2004), Köhler (2008), and IUCN (2024), along with comparisons to those generated in this study, we obtained favorable predictive responses. The distributional patterns are similar to those proposed empirically, with only slight discrepancies.

Honduras possesses a significant expanse of suitable habitat along the Caribbean slope, a characteristic that distinguishes it from other regions within NCA. These similarities with empirical distribution patterns underscore the crucial role of modeling in achieving more accurate delineations and validating boundaries proposed by experts. This approach facilitates the identification of ecological aspects and zones of particular importance crucial for the presence of specific taxa. As previously mentioned, the transition zone in the highlands of the Chortís Block, located between Honduras and Nicaragua, is of particular significance. Consequently, it is imperative to undertake a more profound examination of the influence of biotic and abiotic factors on the distribution and adaptation of various subspecies within this complex. Such studies promise to significantly enhance our

understanding of specialization processes and clarify the taxonomy of this group of coral snakes in Nuclear Central America.

## Acknowledgments

We thank the MHN-UNAH-CU volunteers; Allyson A. Oviedo and for their contributions to the linguistic revision of the manuscript; Ashly M. Gody and Juan C. Hernández for providing us with their laptops for editing figures; and Jose L. Rodríguez Corleto for granting us internet access during the field trip for editing and submission of the manuscript. Additionally, we express our gratitude to two anonymous reviewers for their corrections, comments, and suggestions, which significantly contributed to the manuscript's development, and to editor Jaime Bertoluci for his continuous communication and guidance and finally, Janalee P. Caldwell, for her insightful feedback on the final version of the manuscript. 🐍

---

## References

- ACME Mapper 2.2. 2024. Acme Mapper. Version 2.2. URL <https://mapper.acme.com/>. Captured on 22 July 2024.
- Al Haidar, I. K., A. Ghose, M. Noman, M. M. Rahman, S. Rudra, A. Auawal, R. Islam, A. Uddin, R. A. Efran, A. A. Sayeed, R. Amin, F. Ahsan, A. Faiz, and M. A. Wahed. 2023. Implementation of ecological distribution of venomous snakes for clinical management of snakebite in Bangladesh. *Journal of Medicine* 24: 139–151.
- Allouche, O., A. Tsoar, and R. Kadmon. 2006. Assessing the accuracy of species distribution models: prevalence, Kappa and the true skill statistic (TSS). *Journal of Applied Ecology* 43: 1223–1232.
- Araujo, M. B. and M. New. 2007. Ensemble forecasting of species distributions. *Trends in Ecology and Evolution* 22: 42–47.
- Archis, J. N., C. Akcali, B. L. Stuart, D. Kikuchi, and A. J. Chunco. 2018. Is the future already here? The impact of climate change on the distribution of the eastern coral snake (*Micrurus fulvius*). *PeerJ* 6: 1–25.
- Arenas-Castro, S., A. Regos, and P. González-Moreno. 2022. Modelos de distribución de especies en ecosistemas forestales. Pp. 1–45 in R. M. Navarro, F. J. Mesas, Ó. Pérez, F. J. Ruiz, G. Palacios, P. González-Moreno, and V. Rodríguez (eds.), *Geomática y Ciencia de Datos Aplicadas a la Gestión Forestal: Nuevos Avances y Perspectivas*. Córdoba. Geoforest.
- Banks, P. O. 1975. Basement rocks bordering the Gulf of Mexico and the Caribbean sea. Pp. 181–199 in A. E. M. Nairn and F. G. Stehli. (eds.), *The Gulf of Mexico and the Caribbean*. New York and London. Plenum Press.
- Biber, M. F., A. Voskamp, and C. Hof. 2023. Potential effects of future climate change on global reptile distributions and diversity. *Global Ecology and Biogeography: A Journal of Macroecology* 32: 519–534.
- Breiman, L. 2001. Random Forests. *Machine Learning* 45: 5–32.
- Brineman, J. H. and G. L. Vinson. 1961. Nuclear Central America hub of Antillean transverse belt: abstract. *AAPG Bulletin* 45: 411–412.
- Broennimann, O. and V. Di Cola. 2023. Ecospat: Spatial Ecology miscellaneous methods, an online reference. Electronic Database accessible at <https://cran.r-project.org/web/packages/ecospat/ecospat.pdf>. Captured on 10 April 2023.
- Busby, J. R. 1991. Bioclim: a bioclimate analysis and prediction system. *Plant Protection Quarterly* 6: 8–9.
- Campbell, J. A. and W. W. Lamar (eds.). 2004. *The Venomous Reptiles of the Western Hemisphere*. Ithaca. Comstock Publishing, Cornell University Press. 870 pp.
- Cano, E. B., J. C. Schuster, and J. Morrone. 2018. Phylogenetics of *Ogyges* Kaup and the biogeography of Nuclear Central America (Coleoptera, Passalidae). *ZooKeys* 737: 81–111.
- Carpenter, G., A. N. Gillison, and J. Winter. 1993. DOMAIN: a flexible modelling procedure for mapping potential distributions of plants and animals. *Biodiversity and Conservation* 2: 667–680.
- Cobos, M. E., A. T. Peterson, L. Osorio-Olvera, and D. Jiménez-García. 2019. An exhaustive analysis of heuristic methods for variable selection in ecological niche modeling and species distribution modeling. *Ecological Informatics* 53: 1–10.
- CONABIO (comp). 2023. Catalog of taxonomic authorities of flora and fauna species with distribution in Mexico: an online reference. Electronic Database accessible at <https://www.snib.mx/taxonomia/descarga/>. Captured on 22 February 2023.
- Donnelly, T., G. S. Horne, R. C. Finch, and E. L. Ramos. 1990. Northern Central America; the Maya and Chortís

- blocks. Pp. 1–39 in G. Dengo and J. E. Case (eds.). *The Caribbean Region*. Boulder. Geological Society of America.
- Dormann, C. F., J. Elith, S. Bacher, C. Buchmann, G. Carl, G. Carré, J. R. García-Marquéz, B. Gruber, B. Lafourcade, P. J. Leitão, T. Münkemüller, C. McClean, P. E. Osborne, B. Reineking, B. Schröder, A. K. Skidmore, D. Zurell, and S. Lautenbach. 2013. Collinearity: a review of methods to deal with it and a simulation study evaluating their performance. *Ecography* 36: 27–46.
- Dudík, M., S. J. Phillips, and R. E. Schapire. 2007. Maximum entropy density estimation with generalized regularization and an application to species distribution modeling. *Journal of Machine Learning Research* 8: 1217–1260.
- Elith, J. and J. Franklin. 2013. Species distribution modeling. *Encyclopedia of Biodiversity* 6: 692–705.
- Elith, J. and J. Franklin. 2017. Species Distribution Modeling. *Reference Module in Life Sciences*: 1–15.
- Elith, J. and J. R. Leathwick. 2009. Species distribution models: ecological explanation and prediction across space and time. *Annual Review of Ecology, Evolution, and Systematics* 40: 677–697.
- Elith, J., C. H. Graham, R. P. Anderson, K. M. Dudi, S. Ferrier, A. Guisan, R. J. Hijmans, F. Huettmann, J. R. Leathwick, A. Lehmann, J. Li, L. G. Lohmann, B. A. Loiselle, G. Manion, C. Moritz, M. Nakamura, Y. Nakazawa, J. McC. Overton, A. T. Peterson, S. J. Phillips, K. S. Richardson, R. Scachetti-Pereira, R. E. Schapire, J. Soberon, S. Williams, M. S. Wisz, and N. E. Zimmermann. 2006. Novel methods improve prediction of species' distributions from occurrence data. *Ecography* 29: 129–151.
- Fernández, J., A. Alape, Y. Angulo, L. Sanz, J. M. Gutiérrez, J. J. Calvete, and B. Lomonte. 2011. Venomic and antivenomic analyses of the Central American coral snake, *Micrurus nigrocinctus* (Elapidae). *Journal of Proteome Research* 10: 1816–1827.
- Fick, S. E. and R. J. Hijmans. 2017. WorldClim 2: new 1-km spatial resolution climate surfaces for global land areas. *International Journal of Climatology* 37: 4302–4315.
- Fielding, A. H. and J. F. Bell. 1997. A review of methods for the assessment of prediction errors in conservation presence/absence models. *Environmental Conservation* 24: 38–49.
- Franklin, J. 1995. Predictive vegetation mapping: geographic modelling of biospatial patterns in relation to environmental gradients. *Progress in Physical Geography* 19: 474–499.
- Franklin, J. (ed.). 2009. *Mapping Species Distributions: Spatial Inference and Prediction*. Cambridge. Cambridge University Press. 320 pp.
- Freeman, E. 2023. Presence Absence: Presence-Absence Model Evaluation: an online reference. Electronic Database accessible at <https://cran.r-project.org/web/packages/PresenceAbsence/PresenceAbsence.pdf>. Captured on 10 April 2023.
- Gaige, H. T., N. Hartweg, and L. C. Stuart. 1937. Notes on a collection of amphibians and reptiles from eastern Nicaragua. *Occasional papers of the Museum of Zoology, University of Michigan* 357: 1–18.
- GBIF.org 2023. The Global Biodiversity Information Facility: an Online Reference. Version 278deb0 (26 february 2022). Electronic Database accessible at <https://www.gbif.org>. Captured on 10 February 2023.
- Google. 2023. Google Earth Pro. Version 7.3.2. URL: <https://www.google.com/earth/versions/#earth-pro>.
- Guerra, G. F., L. G. Da Silva, C. Machado, and D. S. Fernandes. 2019. Potential geographic distribution of the genus *Micrurus* Wagler, 1824 (Serpentes: Elapidae) and antivenom supply in Rio de Janeiro state, Brazil. *Oecologia Australis* 23: 496–506.
- Guisan, A. and N. E. Zimmermann. 2000. Predictive habitat distribution models in ecology. *Ecological Modelling* 135: 147–186.
- Guisan, A. and W. Thuiller. 2005. Predicting species distribution: offering more than simple habitat models. *Ecology Letters* 8: 993–1009.
- Guisan, A., R. Tingley, J. B. Baumgartner, I. Naujokaitis-Lewis, P. R. Sutcliffe, A. I. Tulloch, T. J. Regan, L. Brotons, E. McDonald-Madden, C. Mantyka-Pringle, T. G. Martin, J. R. Rhodes, R. Maggini, S. A. Setterfield, J. Elith, M. W. Schwartz, B. A. Wintle, O. Broennimann, M. Austin, S. Ferrier, M. R. Kearney, H. P. Possingham, Y. M. Buckley, and H. Arita. 2013. Predicting species distributions for conservation decisions. *Ecology Letters* 16: 1424–1435.
- Guisan, A., T. C. Edwards, and T. Hastie. 2002. Generalized linear and generalized additive models in studies of species distributions: setting the scene. *Ecological Modelling* 157: 89–100.
- Guisan, A., W. Thuiller. And N. E. Zimmermann (eds.). 2017. *Habitat Suitability and Distribution Models with Applications in R*. Cambridge. Cambridge University Press. 461 pp.
- Guo, Q., M. Kelly, and C. H. Graham, 2005. Support Vector

- Machines for predicting distribution of sudden oak death in California. *Ecological Modelling* 182: 75–90.
- Hernandez, P. A., C. H. Graham, L. L. Master, and D. L. Albert. 2006. The effect of sample size and species characteristics on performance of different species distribution modeling methods. *Ecography* 29: 773–785.
- Hidalgo-García, J. A., J. R. Cedeño-Vázquez, R. Luna-Reyes, and D. González-Solis. 2018. Modelaje de la distribución geográfica de cuatro especies de serpientes venenosas y su percepción social en el sureste de la Altiplanicie de Chiapas. *Acta Zoológica Mexicana* 34: 1–20.
- Hijmans, R. J. 2023. Raster: geographic data analysis and modeling: an online reference. Electronic Database accessible at <https://cran.r-project.org/web/packages/raster/raster.pdf>. Captured on 10 April 2023.
- Hijmans, R. J. and J. Elith. 2017. Species distribution modeling with R: an online reference. Electronic Database accessible at <http://cran.nexr.com/web/packages/dismo/vignettes/sdm.pdf>. Captured on 10 April 2023.
- Hijmans, R. J., S. Phillips, J. Leathwick, and J. Elith. 2023. Dismo: Species Distribution Modeling: an online reference. Electronic Database accessible at <https://cran.r-project.org/web/packages/dismo/dismo.pdf>. Captured on 10 June 2023.
- Holdridge, L. R. (ed.). 1978. *Ecologia: Basada en Zonas de Vida*. San José. Instituto Interamericano de Ciencias Agrícolas. 216 pp.
- Illescas, M. J., M. Dix, and M. L. Maldonado. 2011. *Inventario de Especies de Herpetofauna de las Colecciones Zoológicas en Guatemala. Informe Final: Sistema Guatemalteco de Información Sobre Biodiversidad (SGIB) para la Planificación de Manejo de Vida Silvestre y Áreas Protegidas (Fase IV): Anfíbios y Reptiles*. Guatemala. Proyecto FODECYT (FD18-2006), Secretaría Nacional de Ciencia y Tecnología. 223 pp.
- Interiano, A. L., D. Herrera, H. Orellana-Carrera, R. N. D. Monroy, P. García, J. E. López, and R. A. Jiménez. 2024. Interaction intensity as determinant of geographic range overlap between ant-following birds and army ants. *Neotropical Biology and Conservation* 19: 137–186.
- IUCN (International Union for Conservation of Nature). 2024. The IUCN Red List of Threatened Species. <https://www.iucnredlist.org>. Captured on 16 April 2025.
- James, K. H. 2007. Structural geology: from local elements to regional synthesis. Pp 1–45 in J. Bundschuh and G. E. Alvarado (eds.), *Central America: Geology, Resources and Hazards, Vol. II*. New York. CRC Press, Taylor y Francis Press.
- Jansen, M. and G. Köhler. 2003. Biogeografische Analyse der Herpetofauna von ausgewählten Hochlandgebieten Nicaraguas. *Salamandra* 38: 269–286.
- Johnson, J. D., V. Mata-Silva, E. García-Padilla, and L. D. Wilson. 2015. The herpetofauna of Chiapas, Mexico: composition, physiographic distribution, and conservation status. *Mesoamerican Herpetology* 2: 272–329.
- Jowers, M. J., U. Smart, S. Sánchez-Ramírez, J. C. Murphy, A. Gómez, R. J. Bosque, G. C. Sarker, B. P. Noonan, J. F. Faria, D. J. Harris, N. J. Da Silva, A. L. Prudente, J. Weber, P. J. Kok, G. A. Rivas, R. C. Jadin, M. Sasa, A. Muñoz-Mérida, G. Moreno-Rueda, and E. N. Smith. 2023. Unveiling underestimated species diversity within the Central American coral snake, a medically important complex of venomous taxa. *Scientific Reports* 13: 11674.
- Köhler, G. 2001. *Anfibios y Reptiles de Nicaragua*. Offenbach. Herpeton-Verl. 208 pp.
- Köhler, G. 2003. *Reptiles de Centroamérica*. Offenbach. Herpeton-Verl. 367 pp.
- Köhler, G. 2008. *Reptiles of Central América*. Offenbach. Herpeton-Verl. 393 pp.
- Köhler, G., M. Veselý, and E. Greenbaum. 2006. *The Amphibians and Reptiles of El Salvador*. Malabar. Krieger Publishing. 238 pp.
- Komac, B., P. Esteban, L. Trapero, and R. Caritg. 2016. Modelization of the current and future habitat suitability of *Rhododendron ferrugineum* using potential snow accumulation. *PLoS ONE* 11: 1–18.
- Landy, M. J., D. A. Langebartel, E. O. Moll, and H. M. Smith. 1966. A collection of snakes from Volcan Tacana, Chiapas, México. *Journal of the Ohio Herpetological Society* 5: 93–101.
- Lara-Galván, J. L., M. Montesino-San Martin, J. F. Martínez-Montoya, J. J. Sigala-Rodríguez, J. A. Bañuelos-Alamillo, and M. Barbosa. 2023. Assessing the distribution of the West Mexican Coralsnake, *Micrurus distans* Kennicott, 1860, in Zacatecas State, Mexico, using modelling based on multiple data sources. *Herpetology Notes* 16: 827–836.
- Lippa, E., F. Török, A. Gómez, G. Corrales, D. Chacón, M. Sasa, J. M. Gutiérrez, B. Lomonte, and J. Fernández. 2019. First look into the venom of Roatan Island's critically endangered coral snake *Micrurus ruatanus*: proteomic characterization, toxicity, immunorecognition and neutralization by an antivenom. *Journal of*

- Proteomics* 198: 177–185.
- Lissovsky, A. A., S. V. Dudov, and E. V. Obolenskaya. 2021. Species-distribution modeling: advantages and limitations of its application; 1. General approaches. *Biology Bulletin Reviews* 11: 254–264.
- Mahalanobis, P. C. 1936. On the generalised distance in statistics. *Proceedings of the National Institute of Science of India* 2: 49–54.
- Marques, O. A. V., S. M. Almeida-Santos, and M. G. Rodrigues. 2006. Activity patterns in coral snakes, genus *Micrurus* (Elapidae) in south and southeastern Brazil. *South American Journal of Herpetology* 1: 114–120.
- Marshall, J. S. 2007. The Geomorphology and Physiographic Provinces of Central America. Pp 1–50 in J. Bundschuh and G. E. Alvarado (eds.), *Central America: Geology, Resources and Hazards*. Vol. II. New York. CRC Press, Taylor y Francis Press.
- Martin, G., J. Erinjery, R. Gumbs, R. Somaweera, D. Ediriweera, P. J. Diggle, A. Kasturiratne, H. J. De Silva, D. G. Laloo, T. Iwamura, and K. A. Murray. 2022. Integrating snake distribution, abundance and expert-derived behavioural traits predicts snakebite risk. *Journal of Applied Ecology* 59: 611–623.
- Mata-Silva, V., D. L. DeSantis, E. García-Padilla, D. Jerry, J. D. Johnson, and L. D. Wilson. 2019. The endemic herpetofauna of Central America: a casualty of anthropocentrism. *Amphibian and Reptile Conservation* 13: 1–64.
- Mateo, R. G., Á. M. Felicísimo, and J. Muñoz. 2011. Modelos de distribución de especies: una revisión sintética. *Revista Chilena de Historia Natural* 84: 217–240.
- McCranie, J. R. 2011. The snakes of Honduras: systematics, distribution, and conservation. *Society for the Study of Amphibians and Reptiles* 26: 1–714.
- Mizsei, E., B. Uveges, B. Vági, M. Szabolcs, S. Lengyel, W. P. Pfiögler, Z. T. Nagy, and J. P. Tóth. 2016. Species distribution modelling leads to the discovery of new populations of one of the least known European snakes, *Vipera ursinii graeca*, in Albania. *Amphibia-Reptilia* 37: 55–68.
- Montero, J. M. and J. Velasco. 2024. Herramientas para el análisis en ciencia de datos. Pp. 153–170 in G. Fernández-Avilés and J. M. Montero (eds.), *Fundamentos de Ciencia de Datos con R*. Madrid. McGraw Hill Interamericana de Espana, SL.
- Mota-Vargas, C. and O. R. Rojas-Soto. 2012. The importance of defining the geographic distribution of species for conservation: the case of the Bearded Wood-Partridge. *Journal for Nature Conservation* 20: 10–17.
- Mouton, A. M., B. De Baets, and P. L. Goethals. 2010. Ecological relevance of performance criteria for species distribution models. *Ecological Modelling* 221: 1995–2002.
- Mpakairi, K. S., H. Ndaimani, P. Tagwireyi, T. W. Gara, M. Zvidzai, and D. Madhlamoto. 2017. Missing in action: species competition is a neglected predictor variable in species distribution modelling. *PLoS ONE* 12: 1–14.
- Naimi, B. 2023. usdm: Uncertainty Analysis for Species Distribution Models: an Online Reference. Electronic Database accessible at <https://cran.r-project.org/web/packages/usdm/usdm.pdf>. Captured on 20 April 2023.
- Naimi, B. and M. B. Araújo. 2016. sdm: a reproducible and extensible R platform for species distribution modelling. *Ecography* 39: 368–375.
- Naimi, B. and M. B. Araujo. 2021. sdm: Species Distribution Modelling: an Online Reference. Electronic Database accessible at <https://cran.r-project.org/web/packages/sdm/sdm.pdf>. Captured on 20 April 2023.
- Naimi, B., N. A. S. Hamm, T. A. Groen, A. K. Skidmore, and A. G. Toxopeus. 2013. Where is positional uncertainty a problem for species distribution modelling? *Ecography* 37: 191–203.
- Orellana, S. and Z. López. (eds.). 2023. Portal de Biodiversidad de Guatemala: Digitalización y Manejo de Colecciones Biológicas. Electronic Database accessible at <https://biodiversidad.gt/portal/index.php>, Guatemala. Captured on 30 April 2023.
- Pearson, R. G. 2010. Species' distribution modeling for conservation educators and practitioners. *Lessons in Conservation* 3: 54–89.
- Phillips, S. J. and J. Elith. 2010. POC plots: calibrating species distribution models with presence-only data. *Ecology* 91: 2476–2484.
- Phillips, S. J., M. Dudík, J. Elith, C. H. Graham, A. Lehmann, J. Leathwick, and S. Ferrier. 2009. Sample selection bias and presence-only distribution models: implications for background and pseudo-absence data. *Ecological Applications* 19: 181–197.
- Phillips, S. J., R. P. Anderson, and R. E. Schapire. 2006. Maximum entropy modeling of species geographic distributions. *Ecological Modelling* 190: 231–259.
- Pliscoff, P. and T. Fuentes-Castillo. 2011. Modelación de la distribución de especies y ecosistemas en el tiempo y en el espacio: una revisión de las nuevas herramientas y enfoques disponibles. *Revista de Geografía Norte*

- Grande 48: 61–79.
- Posit Team 2023. RStudio: Integrated Development Environment for R. Version 2023.6.1.524. URL: <http://www.posit.co/>.
- QGIS Development Team. 2023. QGIS un Sistema de Información Geográfica Libre y de Código Abierto. Version 3.28. URL: <http://qgis.osgeo.org>.
- R Core Team. 2023. R: A Language and Environment for Statistical Computing. R. Version 4.3.0. URL: <https://www.R-project.org/>.
- Rodríguez-Gómez, F., Y. Licona-Vera, L. Silva-Cárdenas, and J. F. Ornelas. 2021. Phylogeography, morphology and ecological niche modelling to explore the evolutionary history of Azure-crowned Hummingbird (*Amazilia cyanocephala*, Trochilidae) in Mesoamerica. *Journal of Ornithology* 162: 529–547.
- Roze, J. A. 1967. A check list of the new world venomous coral snakes (Elapidae), with descriptions of new forms. *American Museum Novitates* 2287: 1–60.
- Roze, J. A. 1982. New world coral snakes (Elapidae): a taxonomic and biological summary. *Memórias do Instituto Butantan* 46: 305–338.
- Roze, J. A. 1996. *Coral Snakes of the Americas: Biology, Identification, and Venoms*. Malabar. Krieger Publishing Company. 328 pp.
- Russell, F. E., F. G. Walter, T. A. Bey, and M. C. Fernandez. 1997. Snakes and snakebite in Central America. *Toxicon* 35: 1469–1522.
- Savage, J. M. 1966. The origins and history of the Central American Herpetofauna. *Copeia* 1966: 719–766.
- Schmidt, K. P. 1932. Stomach contents of some American Coral snakes, with the description of a new species of *Geophis*. *Copeia* 1932: 6–9.
- Schmidt, K. P. 1933. Preliminary account of the coral snakes of Central America and México. *Zoological Series of Field Museum of Natural History, Chicago* 20: 29–40.
- Scott, T. L., S. Doucette-Riise, L. A. Obando, and J. H. Townsend. 2011. *Micrurus nigrocinctus* (central American coral snake). Cannibalism. *Herpetological Bulletin* 115: 31–32.
- Segurado, P. and M. B. Araújo. 2004. An evaluation of methods for modelling species distributions. *Journal of Biogeography* 31: 1555–1568.
- Seib, R. L. 1984. Prey use in three syntopic Neotropical racers. *Society for the Study of Amphibians and Reptiles* 18: 412–420.
- Shabani, F., L. Kumar, and M. Ahmadi. 2018. Assessing accuracy methods of species distribution models: AUC, specificity, sensitivity, and the true skill statistic. *Global Journals* 18: 6–18.
- Smith, H. M. and E. H. Taylor. 1945. An annotated checklist and key to the snakes of Mexico. *Bulletin of the United States National Museum* 187: 1–239.
- Stazi, M., F. Fabris, J. Fernández, G. D'Este, M. Rigoni, A. Megighian, J. M. Gutiérrez, B. Lomonte, and C. Montecucco. 2022. Recovery from the neuroparalysis caused by the *Micrurus nigrocinctus* venom is accelerated by an agonist of the CXCR4 receptor. *Toxins* 14: 1–13.
- Stevens, B. S. and C. J. Conway. 2019. Predicting species distributions: unifying model selection and scale optimization for multi-scale occupancy models. *Ecosphere* 10: 1–25.
- Sunyer, J. 2009. Taxonomy, zoogeography, and conservation of the herpetofauna of Nicaragua. Unpublished Doctoral, Dissertation. Goethe University, Frankfurt am Main, Germany.
- Tax, D. M. and R. P. Duin, 2004. Support vector data description. *Machine Learning* 54: 45–6.
- Terribile, L. C., T. C. S. Anacleto, N. J. Silva Jr., and J. A. F. Diniz-Filho. 2007. Potential geographic distribution of the coral snake *Micrurus decoratus* Jan, 1858 (Serpentes, Elapidae) in the Atlantic Rainforest of Brazil. *Arquivos do Museu Nacional* 65: 217–223.
- Thuiller, W., B. Lafourcade, R. Engler, and M. Araujo. 2009. BIOMOD, a platform for ensemble forecasting of species distributions. *Ecography* 32: 369–373.
- Travers, S. L., J. H. Townsend, J. Sunyer, L. A. Obando, L. D. Wilson, and A. N. Max. 2011. New and noteworthy records of amphibians and reptiles from Reserva de la Biósfera Bosawas, Nicaragua. *Herpetological Review* 42: 399–403.
- Van Strien, M. 2008. Best practice species distribution modelling protocol. Version 1.0. Lausanne. Ecospat-Spatial Ecology Group, University of Lausanne.
- Vaughan, I. P. and S. J. Ormerod, 2005. The continuing challenges of testing species distribution models. *Journal of Applied Ecology* 42: 720–730.
- VertNet.org. 2016. Search VertNet: an Online Reference. Version 2016-09-29 (04 July 2020). Electronic database accessible at: <http://portal.vertnet.org/search>. Captured on 28 February 2023.
- Wilson, L. D. and J. R. McCranie. 2004. The conservation status of the herpetofauna of Honduras. *Amphibian and*

*Reptile Conservation* 3: 6–33.

Worldclim.org. 2023. WorldClim: an Online Reference. Version 2020-2022. Electronic Database accessible at <https://www.worldclim.org/data/index.html>. Captured on 17 April 2023.

Zhang, J. and S. Li. 2017. A review of Machine Learning Based Species' Distribution Modelling. Pp. 199–206 in J. E. Guerrero (ed.), *2017 International Conference on Industrial Informatics, Computing Technology, Intelligent Technology, Industrial Information Integration (ICIICII)*. Wuhan. IEE Computer Society, Conference Publishing Services (CPS).

Zhang, L., S. Liu, P. Sun, T. Wang, G. Wang, X. Zhang, and L. Wang. 2015. Consensus forecasting of species distributions: the effects of niche model performance and niche properties. *PLoS ONE* 10: 1–18.

Zurell, D., J. Franklin, C. König, P. J. Bouchet, C. F. Dormann, J. Elith, G. Fandos, X. Feng, G. Guillera-Arroita, A. Guisan, J. J. Lahoz-Monfort, P. J. Leitão, D. S. Park, A. T. Peterson, G. Rapacciuolo, D. R. Schmatz, B. Schröder, J. M. Serra-Diaz, W. Thuiller, K. L. Yates, N. E. Zimmermann, and C. Merow 2020. A standard protocol for reporting species distribution models. *Ecography* 43: 1261–1277.

Editor: Jaime Bertolucci

**Appendix I.** Historical records of the *Micrurus divaricatus* species complex, along with their geographical references in decimal degrees format, are used as presence data. Data are presented as Code (latitude, longitude).

**El Salvador; Köhler et al. 2006:** 1 (13.93098, -89.81564), 2 (13.71667, -88.93333), 3 (13.85, -88.96667), 4 (13.83333, -88.98056), 5 (13.64949, -89.26276), 6 (13.87487, -89.37644), 7 (14.2791, -89.45), 8 (13.696969, -89.233333), 9 (13.686482, -89.177341), 10 (13.745379, -89.669616), 11 (13.83333, -89.96666), 12 (13.283333, -88.55), 13 (13.199025, -88.053147), 14 (14.38087, -89.399929), 15 (13.88374, -88.963933), 16 (13.829419, -88.147227), 17 (13.832662, -89.520137), 18 (13.81905, -89.576632), 19 (13.31957, -88.63889).

**Guatemala; Orellana, S. and Z. López. (eds.). 2023:** 20 (14.7028, -91.8611), 21 (14.6042, -90.5806), 22 (14.6556, -91.8247), 23 (14.0811, -91.0522), 24 (14.733333, -91.15), 25 (14.152309, -90.26342), 26 (14.75, -91.166667), 27 (14.746946, 91.128027), 28 (14.816667, -91.833333), 29 (14.190873, -90.433333), 30 (14.133333, -90.283333), 31 (14.75508, -91.149313), 32 (14.812773, -91.829879), 33 (14.6065, -90.4901), 34 (14.5511, -90.5772), 35 (14.5, -90.9542), 36 (14.3814, -90.4306), 37 (14.5511, -90.5772), 38 (14.8167, -91.9167), 39 (14.6247, -90.4494), 40 (15.0017, -89.6583), 41 (14.4783, -90.6189), 42 (14.6941, -89.3485), 43 (13.8028, -90.1956), 44 (14.6389, -89.4376), 45 (14.5967, -91.7264), 46 (14.3328, -89.7094), 47 (14.6425, -91.7344).

**Honduras; McCranie 2011:** 48 (14.8333, -89.15), 49 (14.5833, -88.5833), 50 (14.9, -89.0333), 51 (14.9194, -87.9771), 52 (13.85, -86.6833), 53 (14.0667, -86.55), 54 (15.0333, -85.9), 55 (15.1333, -84.4), 56 (15.8, -84.3), 57 (14.9333, -84.5333), 58 (14.8667, -84.65), 59 (14.8167, -84.8667), 60 (15.6167, -87.3167), 61 (15.9, -85.95), 62 (14.041316, -87.045327), 63 (14.07, -86.1), 64 (15.4167, -88.15), 65 (15.8235, -87.30032), 66 (14.4667, -87.65), 67 (15.77, -86.6833), 68 (15.3833, -86.2167), 69 (14.0333, -86.5667), 70 (15.0833, -85.5667), 71 (15.0167, -84.2167), 72 (15.5167, -88.2), 73 (15.1167, -86.7667), 74 (14.9406, -88.0146), 75 (14.1, -86.7333), 76 (15.4, -87.8), 77 (14.0, -87.0167), 78 (15.45, -85.0833), 79 (15.7, -86.85), 80 (15.7167, -85.95), 81 (15.7167, -87.76), 82 (14.95, -84.6667), 83 (13.3333, -87.6167), 84 (14.9333, -84.6667), 85 (15.05, -84.8833), 86 (15.781249, -86.786535), 87 (14.95, -85.8833), 88 (15.4167, -87.3167), 89 (15.4333, -87.9167), 90 (14.05, -86.4833), 91 (15.55, -87.8833), 92 (15.7333, -87.45), 93 (15.0667, -84.8333), 94 (14.0333, -86.95), 95 (14.15475, -87.1513), 96 (15.6167, -86.7667), 97 (13.9833, -86.4833), 98 (14.75, -84.45), 99 (15.0167, -84.2833), 100 (15.1333, -86.7333), 101 (14.2886, -86.85), 102 (15.2, -87.3667), 103 (14.9667, -88.0167), 104 (14.8833, -85.9), 105 (15.0833, -87.3333), 106 (15.7667, -87.499993), 107 (15.6333, -86.7833), 108 (15.1167, -86.7333), 109 (15.3167, -85.2833), 110 (15.1, -84.4333), 111 (15.3833, -86.25), 112 (15.6667, -86.7), 113 (14.7167, -84.45), 114 (13.4167, -87.45), 115 (13.4333, -86.8167), 116 (15.5, -88.0333), 117 (14.95, -84.5167), 118 (15.6333, -87.05), 119 (14.7833, -84.4833), 120 (15.3, -83.8833), 121 (14.85, -84.53333333), 122 (14.1, -87.2), 123 (15.2, -86.7), 124 (15.0167, -84.65), 125 (15.7167, -87.7667), 126 (15.91636, -85.94941), 127 (15.7333, -87.6167), 128 (14.9167, -84.6833), 129 (15.35, -84.2333), 130 (14.9167, -84.6833), 131 (15.44669964, -87.78699951), 132 (14.0573, -87.2114), 133 (15.85, -87.9333), 134 (15.954053, -85.90452).

**Mexico; CONABIO (comp). 2023:** 135 (15.0372394, -92.1452034), 136 (15.08611, -92.09028), 137 (15.36, -92.23), 138 (15.347222, -92.693889), 139 (16.661111, -93.565278), 140 (15.083333, -92.252222), 141 (16.188611, -93.918056), 142 (16.138806, -93.614055), 143 (15.479167, -92.846667), 144 (15.41, -92.63), 145 (16.83, -93.19), 146 (16.7080556, -93.0133333), 147 (15.365278, -92.644444), 148 (15.3625, -92.654167), 149 (15.441667, -92.641667), 150 (15.384722, -92.609722).

Appendix I. Continued.

Nicaragua; Köhler 2001, Sunyer 2009: 151 (12.955222, -85.230889), 152 (11.3080278, -85.9164167), 153 (11.324154, -85.711263), 154 (11.844167, -85.988056), 155 (11.816667, -85.966667), 156 (12.041868, -86.155722), 157 (12.008864, -86.287994), 158 (14.3535, -84.942), 159 (12.918273, -85.884966), 160 (11.29972, -85.764063), 161 (12.474348, -87.076823), 162 (14.296217, -84.918517), 163 (13.738586, -84.784889), 164 (14.387767, -84.979917), 165 (11.172778, -84.990833), 166 (13.728917, -84.887361), 167 (14.355833, -84.947778), 168 (14.498056, -84.9475), 169 (13.585518, -85.704848), 170 (14.456931, -85.177629), 171 (13.011389, -85.236556), 172 (13.22, -86.330833), 173 (13.734722, -85.018056), 174 (13.01, -85.988056), 175 (13.61963, -85.72331), 176 (14.459847, -84.981499), 177 (14.36533, -84.93495), 178 (11.43716, -85.82633).

Appendix II. Analysis for the selection of test data, based on the AUC, the TSS, and the COR, for the different models considered. The values presented in bold are of greater magnitude.

RF	AUC <sub>mean</sub>	TSS <sub>mean</sub>	COR <sub>mean</sub>	MAH	AUC <sub>mean</sub>	TSS <sub>mean</sub>	COR <sub>mean</sub>
Data <sub>test</sub> 20	0.97182	0.85728	0.84672	Data <sub>test</sub> 20	<b>0.9174</b>	<b>0.6989</b>	<b>0.3657</b>
Data <sub>test</sub> 25	0.97203	0.85819	0.84711	Data <sub>test</sub> 25	0.9155	0.6978	0.3605
Data <sub>test</sub> 30	<b>0.97373</b>	<b>0.86438</b>	<b>0.85175</b>	Data <sub>test</sub> 30	0.9133	0.6933	0.3610
Data <sub>test</sub> 35	0.97151	0.86135	0.84840	Data <sub>test</sub> 35	0.9095	0.6777	0.3576
Data <sub>test</sub> 40	0.97227	0.86030	0.84849	Data <sub>test</sub> 40	0.9149	0.7027	0.3640
SVM	AUC <sub>mean</sub>	TSS <sub>mean</sub>	COR <sub>mean</sub>	MAH	AUC <sub>mean</sub>	TSS <sub>mean</sub>	COR <sub>mean</sub>
Data <sub>test</sub> 20	0.91274	0.72769	0.71894	Data <sub>test</sub> 20	0.8044	0.5820	0.5039
Data <sub>test</sub> 25	0.91470	0.73157	0.72311	Data <sub>test</sub> 25	0.8048	0.5840	0.5043
Data <sub>test</sub> 30	0.91453	0.72854	0.72212	Data <sub>test</sub> 30	0.8044	0.5834	0.5035
Data <sub>test</sub> 35	0.91447	0.73125	0.72281	Data <sub>test</sub> 35	<b>0.8082</b>	<b>0.5897</b>	<b>0.5100</b>
Data <sub>test</sub> 40	<b>0.91540</b>	<b>0.73182</b>	<b>0.72485</b>	Data <sub>test</sub> 40	0.8043	0.5818	0.5035
GAM	AUC <sub>mean</sub>	TSS <sub>mean</sub>	COR <sub>mean</sub>	MAH	AUC <sub>mean</sub>	TSS <sub>mean</sub>	COR <sub>mean</sub>
Data <sub>test</sub> 20	0.87562	0.69883	0.68402	Data <sub>test</sub> 20	0.7186	0.3937	0.3770
Data <sub>test</sub> 25	0.87274	0.69094	0.67934	Data <sub>test</sub> 25	0.7202	0.3948	0.3797
Data <sub>test</sub> 30	0.87644	0.68765	0.68765	Data <sub>test</sub> 30	0.7181	0.3925	0.3770
Data <sub>test</sub> 35	<b>0.87848</b>	<b>0.70516</b>	<b>0.69000</b>	Data <sub>test</sub> 35	<b>0.7219</b>	<b>0.3990</b>	<b>0.3812</b>
Data <sub>test</sub> 40	0.87689	0.69725	0.68092	Data <sub>test</sub> 40	0.7195	0.3950	0.3781
MaxEnt	AUC <sub>mean</sub>	TSS <sub>mean</sub>	COR <sub>mean</sub>	MAH	AUC <sub>mean</sub>	TSS <sub>mean</sub>	COR <sub>mean</sub>
Data <sub>test</sub> 20	0.88535	0.68305	0.66135	Data <sub>test</sub> 20	0.4264	0.7305	0.2810
Data <sub>test</sub> 25	0.88934	0.69280	0.66690	Data <sub>test</sub> 25	0.4271	0.7290	0.2767
Data <sub>test</sub> 30	0.88462	0.68475	0.65757	Data <sub>test</sub> 30	<b>0.4280</b>	<b>0.7317</b>	<b>0.2865</b>
Data <sub>test</sub> 35	0.88865	0.68230	0.66361	Data <sub>test</sub> 35	0.4269	0.7286	0.2795
Data <sub>test</sub> 40	<b>0.88881</b>	<b>0.69639</b>	<b>0.66743</b>	Data <sub>test</sub> 40	0.4272	0.7302	0.2849

**Appendix III.** Suggested ranges for the seven variables used in model generation. Values for variables that significantly influenced distribution of the *Micrurus divaricatus* complex are highlighted in bold.

	BIO2		BIO4		BIO9		BIO12		BIO14		BIO15		BIO18	
	Min	Max	Min	Max	Min	Max	Min	Max	Min	Max	Min	Max	Min	Max
SVM	7.5	10.5	<b>63.4</b>	<b>135.9</b>	18.9	24.3	899.1	424.2	<b>1.4</b>	<b>83.8</b>	<b>40.5</b>	<b>112.3</b>	246.5	678.9
MaxEnt	7.7	12.8	<b>43.3</b>	<b>121.8</b>	18.6	28.8	899.1	2828.5	<b>1.4</b>	<b>30.3</b>	<b>40.5</b>	<b>75.3</b>	123	913
GAM	10.7	8.4	<b>105.7</b>	<b>55.3</b>	20.1	28.8	817	2335.9	<b>1.4</b>	<b>24.5</b>	<b>41.9</b>	<b>63</b>	123	133.6
RF	8.4	12.5	<b>55.3</b>	<b>115.7</b>	20.5	27.7	1309.6	1761.2	<b>1.4</b>	<b>78</b>	<b>40.5</b>	<b>70.2</b>	209.5	456.5